CHEMISTRY
A EUROPEAN JOURNAL

ChemPubSoc
Europe

DOI: 10.1002/chem.201204529

General Synthesis and Physicochemical Characterisation of a Series of Peptide-Mimic Lysine-Based Amino-Functionalised Lipids

Christian Wölk,[a] Simon Drescher,[a] Annette Meister,[b] Alfred Blume,[b] Andreas Langner,[a] and Bodo Dobner*[a]

Abstract: A series of novel malonic acid diamides (second generation) with two long hydrophobic alkyl chains and an alkaline polar head group was synthesised and characterised as a new class of amino-functionalised lipids. These peptide-mimic lipids are suitable for polynucleotide transfer. The lipids bear a novel backbone consisting of a lysine unit and a malonic acid unit. Six different head-group structures, which vary in size and number of amino groups that can be protonated, were attached to the backbone structure. Furthermore, different alkyl chains were used to build the lipophilic part (namely tetradecyl, hexadecyl, and oleyl). Phase transitions of the new compounds in aqueous dispersions at pH 10 were analysed and discussed in terms of head group and alkyl chain variations. The shape and size of the formed aggregates of selected lipid dispersions were investigated by dynamic light scattering and transmission electron microscopy.

Keywords: amides · lipids · phase transitions · self-assembly · synthetic methods

Introduction

Amino-functionalised and cationic lipids offer various applications in the field of medicine. For example, they are used as non-viral nucleic acid delivery systems,[1] drug-delivery systems for neoplastic diseases[2] and, more recently, as vaccine carriers or adjuvants.[3] Furthermore, their use as antimicrobial agents is described.[4] During the last two decades the application of alkaline or cationic lipids as nucleic acid delivery systems (nucleic acid delivery with lipids is called "lipofection") gained great importance. Within classical gene therapy, which means the treatment of diseases through the use of DNA-based drugs allowing the delivery of DNA to cells followed by expression of a therapeutic gene, cationic lipids are common and widely used delivery systems besides cationic polymers and viral vectors.[1a,5] Additionally, the methods of gene silencing using antisense oligonucleotides and siRNA,[6] respectively, are applications for amino-functionalised lipids. At present, viral vectors are the most-used nucleic acid delivery systems.[7] However, fundamental problems are associated with viral vector systems, namely toxicity, immunogenicity and limitations with respect to scale-up procedures.[8] Due to these disadvantages synthetic chemical vectors became a promising alternative, and the lipid-based vectors are the most-used representatives of this group.[7,8b,9]

Recently, we reported on a new class of amino-functionalised lipids with a malonic acid diamide structure as backbone and two hydrophobic alkyl chains.[10] Therein, we varied the hydrophobic molecule part and the head-group region of the lipids with the aim to gain information about structure-function relationships. Within that previous work, some very effective amino-functionalised lipids have been prepared exceeding commercially available synthetic vectors, such as Lipofectamine, in their transfection efficacy. Furthermore, selected lipid-based vectors of these novel cytofectines have been investigated by physicochemical methods, such as X-ray scattering, differential scanning calorimetry (DSC) and Langmuir film balance measurements, which explained the observed structure–activity relationships.[11]

Herein, we describe the synthesis of a series of malonic acid diamides with a modified backbone (called second generation) based on a malonic acid structure combined with a lysine unit (Figure 1). The hydrophobic part contains two long alkyl chains of variable length and saturation (tetradecyl, hexadecyl, and oleyl chains); the first alkyl chain is bound through an amide bond to the lysine unit and the second one is bound to the α-carbon of the malonic acid unit, thus resulting in a larger distance of the alkyl chains in comparison to the alkyl chains in glycerol-based phospholipids. Due to the complexity of the transfection pathway, no general schemes have emerged correlating the structure of amino-functionalised/cationic lipids with their transfection efficacy and, hence, the approaches for optimising the struc-

[a] Dipl.-Pharm. C. Wölk, Dr. S. Drescher, Prof. Dr. A. Langner, Prof. Dr. B. Dobner
Institute of Pharmacy, MLU Halle-Wittenberg
Wolfgang-Langenbeck-Strasse 4, 06120 Halle/Saale (Germany)
Fax: (+49) 345-55-27018
E-mail: bodo.dobner@pharmazie.uni-halle.de

[b] Dr. A. Meister, Prof. Dr. A. Blume
Institute of Chemistry, MLU Halle-Wittenberg
Von-Danckelmann-Platz 4, 06120 Halle/Saale (Germany)

Supporting information for this article is available on the WWW under http://dx.doi.org/10.1002/chem.201204529. It contains further experimental details and the detailed characterisation of the lipid precursors **9a–c**, **11a–c**, **12a–c**, **13a–c**, **15a–c**, and **16a–c**.

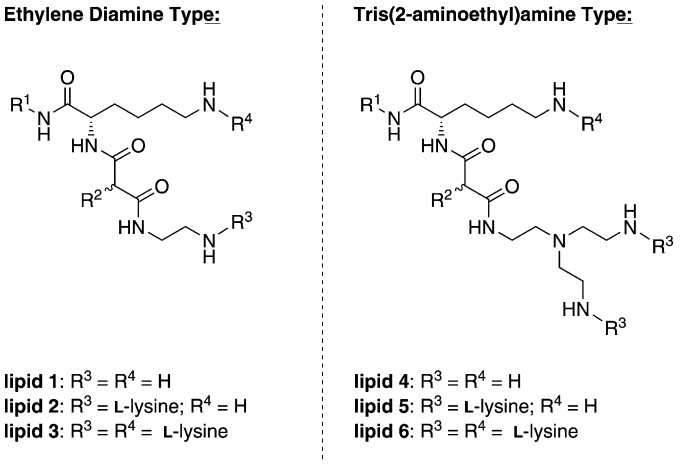

Figure 1. Chemical structures and abbreviations of the 18 malonic acid diamides synthesised in this work.

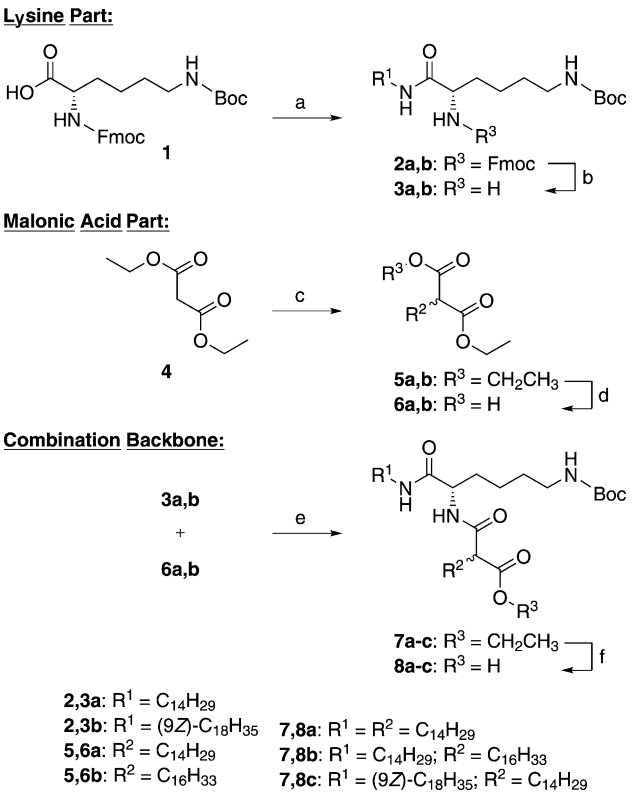

Scheme 1. Synthesis of the lipid backbone: a) tetradecylamine/oleylamine, PyBOP, DIPEA, CH_2Cl_2, RT; b) piperidine, DMF; c) tetradecyl bromide/hexadecyl bromide, NaH, toluene; d) 1) KOH, ethanol, RT; 2) HCl, H_2O; e) PyBOP, DIPEA, CH_2Cl_2, RT; f) 1) KOH, THF, H_2O; 2) H_2SO_4, H_2O. See text for details.

ture of these lipids are still largely empirical. To close this gap, we varied the head-group volume of our lipids by using different spacers (ethylenediamine type, tris(2-aminoethyl)-amine type), and different numbers of coupled lysines (zero to three). We chose the amide bond as the main connecting bond between the different building blocks of the lipid because of its biodegradability (which is necessary for low toxicity),[12] and its higher stability to hydrolysis compared with the ester bond. Furthermore, we used the proteinogenic amino acid lysine as a main unit for the head group and the backbone, because of its biocompatibility and known ability to form complexes with DNA as a main element of histones and poly-L-lysine.[13] The structural modifications result in 18 novel amino-functionalised lipids with peptide-like structure elements (peptide-mimic lipids, Figure 1).

The main focus of this work is the detailed description of the lipid synthesis. Furthermore, the report summarises the chemical and physicochemical properties of the novel lipids. We investigated the pure aqueous lipid dispersions at pH 5 and 10 by means of DSC to obtain information about the thermal behaviour of the pure lipids and to explore the influence of structural variations in the lipophilic part and the head-group region of the molecules on the thermal behaviour. In addition, we investigated the formed aggregate structures of selected aqueous lipid dispersions at pH 10 by means of dynamic light scattering (DLS) and transmission electron microscopy (TEM).

Results and Discussion

Synthetic methods: The synthetic strategy developed in this work allows easy variation of the alkyl chains by different combinations of separately prepared molecule parts. Scheme 1 describes the synthesis of the lipid backbone. The starting material was the orthogonally amine-protected L-lysine derivative **1** with an amine labile 9-fluorenylmethoxycarbonyl (Fmoc) protective group in the α position and an acid labile *tert*-butoxycarbonyl (Boc)-protected amino group in the ε position. Compound **1** was first coupled with tetradecylamine and oleylamine with (benzotriazol-1-yloxy)tripyrrolidinophosphonium hexafluorophosphate (PyBOP) as coupling agent and diisopropylethylamine (DIPEA) as accessory base, yielding the orthogonally protected lysine amides **2** (yield: 72–82%). The property that DIPEA cleaves the Fmoc group very slowly in comparison with other tertiary amines (50% DIPEA in dimethylformamide (DMF): $t_{1/2}=10.1$ h[14]) ensures its application as proton catching agent for this coupling reaction. PyBOP is an effective coupling agent for the synthesis of amides successfully used in peptide synthesis.[15] Afterwards, the Fmoc deprotection of compounds **2** with piperidine yields the ε-Boc-protected lysine derivatives **3** with a free α-amino group needed for a further amide coupling reaction. Piperidine cleaves the Fmoc group very fast (20% in DMF: $t_{1/2}=3$ s; 5% in DMF: $t_{1/2}=20$ s[14]). In addition, we also used DMF as solvent, according to the Merrifield peptide synthesis technique.[16]

The starting material for the synthesis of the second part of the backbone was the malonic acid diethyl ester **4**, which was transformed into the monoalkylated derivatives **5** by

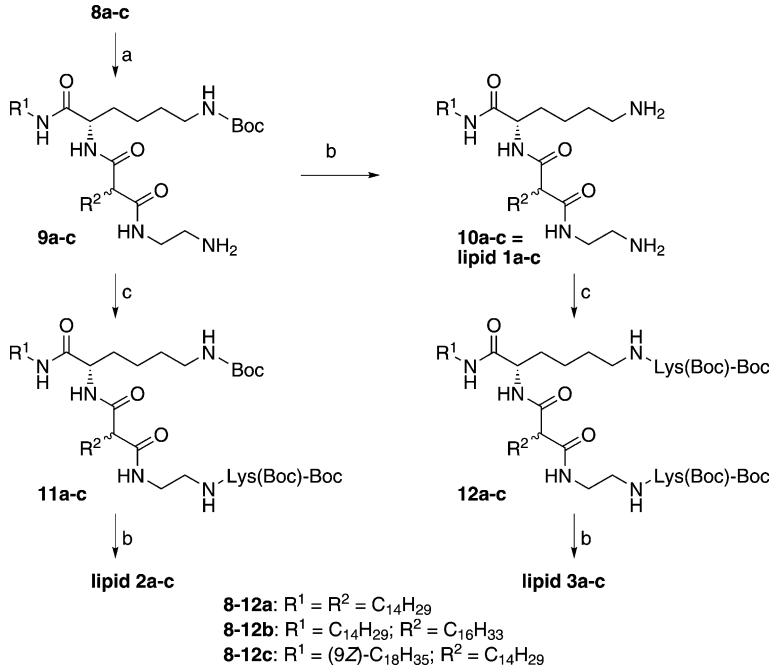

Scheme 2. Synthesis of the lipids with an ethylenediamine moiety: a) ethylenediamine, PyBOP, TEA, CH_2Cl_2; b) 1) TFA, CH_2Cl_2; 2) H_2O, NH_3; c) Boc-Lys(Boc)-OSu, TEA, CH_2Cl_2.

treatment with sodium hydride and tetradecyl and hexadecyl bromide. This reaction is described in various procedures,[17] but our experience showed that the use of toluene as solvent and sodium hydride as deprotonating agent gave the best results. The following monosaponification step by using potassium hydroxide yields the malonic acid monoethyl esters **6**.[18] The two backbone parts **3** and **6** can readily be prepared in higher quantities (up to 10 g). A different combination of both parts in the following amide coupling step allows an easy alkyl chain variation, which opens the way for a wide spectrum of lipids for further structure–function relationship studies. The carboxylic acids **6** and the amines **3** were coupled with PyBOP/DIPEA, resulting in the formation of the amides **7** (yield: 93–97%). We used DIPEA in this coupling reaction because of its increasing effect on the yields in sterically hindered reactions.[19] In a further saponification step the ethyl ester function of compounds **7** was converted into the free carboxylic acid of compounds **8**. This reaction was carried out under mild conditions by using only an excess of potassium hydroxide of 0.5 equivalents with regard to compounds **7**.

The synthesis of the head-group region was designed in such a way that the number of free amino groups that can be protonated and, hence, the resulting volume of the head group could be easily varied for further structure-activity relationship studies. For this purpose, the lipid backbone prepared so far offers two connecting positions for the amino-functionalised head group: on the one hand, the ε-amino group of the lysine, which can be coupled with various carboxylic acids, and on the other hand, the free carboxylic acid moiety of the malonic acid unit that can be connected with different amines. Thus, the lipid backbone consists, in principle, of two different head groups, which can be synthesised and connected separately allowing a huge variety of structures.

The free carboxylic acid moiety of compounds **8** can be coupled with either ethylenediamine, resulting in the **lipids 1–3a–c**, or with tris(2-aminoethyl)amine, yielding **lipids 4–6a–c**. Both amine spacers further increase the structural diversity of the lipids prepared in this work.

The synthesis of **lipids 1–3a–c**, which contain ethylenediamine as spacer, is described in Scheme 2. The carboxylic acids **8** were coupled with ethylenediamine through amide bond formation by using PyBOP and triethylamine (TEA). This reaction step needs no monoprotection of the ethylenediamine due to the large excess (about 20 equiv) of ethylenediamine used in this coupling reaction. After chromatographic purification, the resulting compounds **9** were treated with trifluoroacetic acid (TFA) to cleave the Boc groups and to yield compounds **10** (**lipids 1a–c**) that contain the smallest head group, with two amino moieties that can be protonated. For a further enlargement of the head-group region we used the Boc-protected *N*-hydroxysuccinimide ester of the proteinogenic amino acid L-lysine (Boc-Lys(Boc)-OSu)—an activated amide bond forming ester successfully used in peptide synthesis.[20] Compounds **9**, as well as **10**, were coupled with one or two molecules of Boc-Lys(Boc)-OSu, resulting in the formation of the Boc-protected compounds **11** and **12**, respectively. The subsequent cleavage of the Boc groups with TFA yields **lipids 2a–c**, with three amino groups, and **lipids 3a–c**, bearing four amino groups. The final purification of **lipids 1–3a–c** was carried out with column chromatography on silica gel and a gradient technique by using chloroform, methanol, and ammonia as eluents.

For the synthesis of **lipids 4–6a–c**, we used tris(2-aminoethyl)amine instead of ethylenediamine as spacer to finally increase the number of amino groups that can be protonated and, hence, to enlarge the head-group region. The synthetic procedures are comparable to the aforementioned syntheses (Scheme 3). Starting from compounds **8**, the amidation of the carboxylic acid moieties with tris(2-aminoethyl)amine by using PyBOP/TEA led to the formation of compounds **13**. After the subsequently performed cleavage of the Boc group, compounds **14** (**lipids 4a–c**) were obtained. Both compounds **13** and **14** were used for the coupling with different numbers of lysine residues, leading to compounds **15**

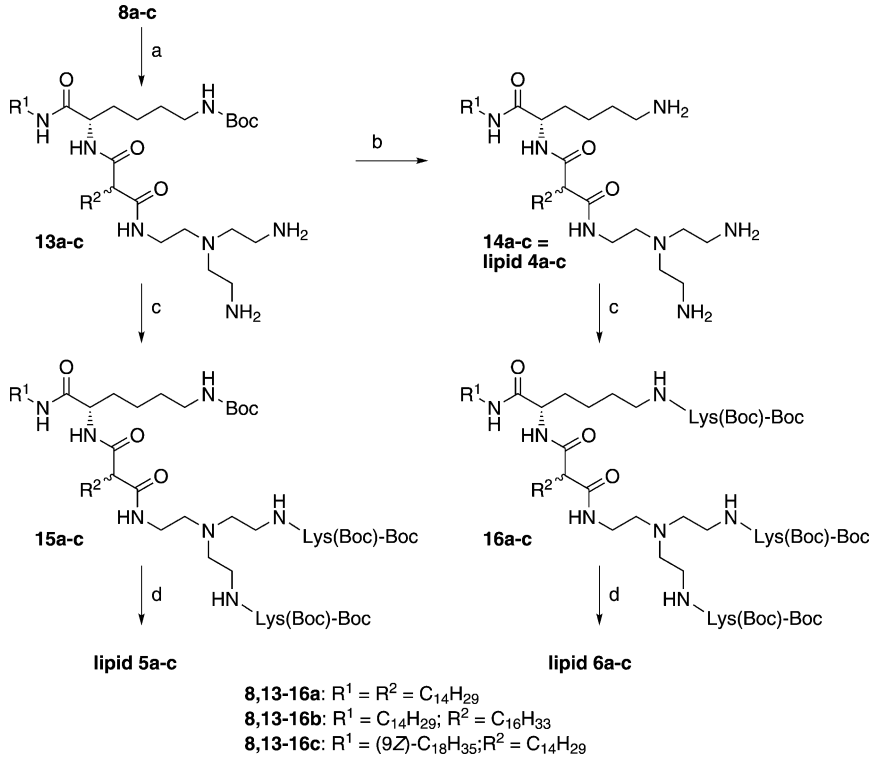

Scheme 3. Synthesis of the lipids with a tris(2-aminoethyl)amine moiety: a) tris(2-aminoethyl)amine, PyBOP, TEA, CH_2Cl_2; b) 1) TFA, CH_2Cl_2; 2) H_2O, NH_3; c) Boc-Lys(Boc)-OSu, TEA, CH_2Cl_2; d) 1) HCl, H_2O, ethyl acetate; 2) DMAP, $CHCl_3$, methanol.

and **16**, respectively. For the final cleavage of the Boc moieties of **15** and **16**, we used a modified method because the TFA salts, which were achieved with the generally applied method, were difficult to work up. Instead, we used hydrochloric acid as the cleaving agent. Normally, HCl-saturated organic solvents, for example, ethyl acetate, are appropriate for this purpose,[21] but due to the easier handling we utilised aqueous HCl, as described previously.[22] Additionally, we worked with a two-phase system containing water and ethyl acetate as solvents because of the insolubility of the Boc-protected compounds in water. A comparable procedure was previously described for a toluene–water–HCl system.[23] Furthermore, we used a novel method of workup: after the deprotection of the amino moieties of **lipids 5a–c** and **6a–c**, we added 4-dimethylaminopyridine (DMAP) to the dissolved lipid–HCl salts and purified this mixture by column chromatography (see the Experimental Section, method b, yield: 97–99%). This technique eliminates the washing steps, which are connected with enormous loss of substance due to the high hydrophilicity of **lipids 5a–c** and **6a–c** (see the Experimental Section, method a, yield: 21–27%). In this procedure, DMAP acts as a strong base and yields the free amino groups through transprotonation. During column chromatography (by using the gradient technique and chloroform, methanol, and ammonia as eluents), the resulting DMAP–HCl was eluted first as a lipophilic ion pair, followed by the **lipids 5a–c** and **6a–c**.

This module-like synthesis strategy allows a straightforward combination of different alkyl chains with diverse head groups, which are variable in size and number of amino groups, thereby resulting in a series of amino-functionalised lipids applicable for further structure influence investigations.

Stereochemical investigations: To achieve biocompatibility of the lipids, we used the proteinogenic amino acid L-lysine within the lipid backbone and head group. Hence, we had to pay attention to the stereochemistry of the amino acid units. We applied the commercially available Boc-Lys(Boc)-OSu exhibiting an *S* configuration for the lysine coupling reaction. The coupling methods with *N*-hydroxysuccinimide esters are described to be free of racemisation.[24] In addition, the coupling reaction by using PyBOP is nearly free of racemisation.[25] Furthermore, we chose every reaction step so that we used only reaction conditions that do not cause amino acid racemisation, that is, the protective group cleaving agents were used under conditions that are common in peptide synthesis, and the saponification reactions in the presence of amino acid moieties were performed under mild conditions. Therefore, we can assume that all of the lysine moieties in the lipids are *S* configured.

Surprisingly, the cleavage of Boc groups resulted in the formation of two different substances if the product mixture was investigated by thin-layer chromatography (TLC). However, ESI-MS measurements of these two substances, obtained by preparative TLC, showed the same mass spectra of the desired product. With regard to the synthetic pathway, we conclude the formation of diastereomers: the alkyl amide of the Boc-protected derivative of L-lysine (**3**) and the racemate of the alkylated malonic acid monoethyl ester (**6**) were connected by the formation of a rigid amide bond resulting in two diastereomers with *SR* and *SS* configuration. At first we tried to separate both diastereomers by column chromatography, but purification could not be realised, although the R_f values of the two substances indicated a distinct separation. Surprisingly, the extraction of one diastereomer from the TLC plate resulted again in two spots in a second TLC run, which reflected the "in situ" formation of the pair of diastereomers (see the Supporting Information). This indicates that the stereocentre at the α carbon of the malonic acid unit racemises in the alkaline milieu of the

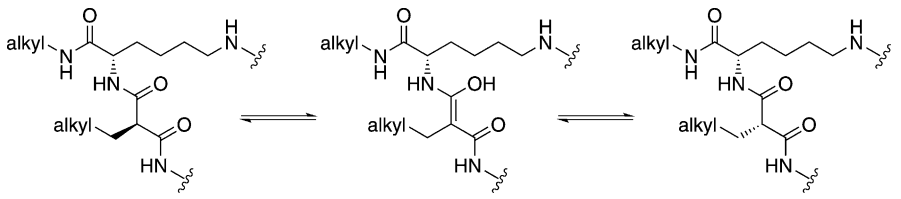

Scheme 4. Postulated mechanism for the stereocentre racemisation at the malonic acid moiety of the lipids.

mobile phase during chromatography, which is also an explanation for our inability to separate the mixture. Scheme 4 shows a possible mechanism of the diastereomer transformation, including an enol as the intermediate structure.

For further investigations with respect to detailed physicochemical properties, polynucleotide binding properties, and gene transfer efficiencies (results will be published elsewhere), we will take into account the presence of two diastereomers.

Nuclear magnetic resonance investigations: All novel lipids (**lipids 1–6a–c**) were investigated by ^{1}H and ^{13}C NMR measurements. The general ^{1}H NMR spectra of our lipids are similar to those obtained from polymers. This is due to the complex molecular structures exhibiting a large number of protons with comparable chemical shifts. The NMR characteristics of the amide groups, such as anisotropy and *cis–trans* isomerism, further complicate the spectra.[26] Hence, it is quite demanding to interpret ^{1}H NMR spectra on the basis of signal splitting and coupling constants. However, with the use of H,H COSY measurements, we were able to interpret the ^{1}H NMR spectra (examples of ^{1}H NMR and H,H COSY spectra are shown in the Supporting Information). For NMR measurements, the lipids were normally dissolved in $CDCl_3$. Surprisingly, some of our lipids showed the formation of a transparent organo-gel, which is further connected with an extensive broadening of the proton signals. A decrease of the lipid concentration or the addition of small amounts of CD_3OD (which is able to break the hydrogen bonds between the lipids) led to the breakdown of the gel. However, the signal intensity and the comparability of the spectra were affected; for example, methanol can shift some ^{1}H NMR signals to higher/lower ppm values and almost all NH ^{1}H NMR signals are lost with the use of methanol. Surprisingly, the **lipids 6a–c** and **lipid 5b**, which have a large head group, are insoluble in common NMR solvents, except D_2O. Therefore, we had to carry out the ^{1}H NMR spectroscopy in D_2O at higher temperatures, at which the signals are narrower, because the lipid structures in water become more fluid.

^{13}C NMR measurements were carried out in $CDCl_3$/CD_3OD mixtures (except the insoluble lipids, for which D_2O was used). As the ^{13}C NMR spectra of our lipids are also very complex, we could only assign related carbon NMR signal groups with carbon-atom groups bearing a related chemical shift (e.g., carbonyl carbon atoms; see the Experimental Section; examples for ^{13}C NMR and C,H COSY are shown in the Supporting Information). In addition, we observed a strong solvent dependency of the chemical shift and the number of ^{13}C NMR signals. In Figure 2, two regions of ^{13}C NMR spectra of **lipid 1c** are shown with various solvents and lipid concentrations. Figure 2F (39–56 ppm: CH_2NHCO, CH_2NH_2, COCHR-CO and lysine α carbon) shows the signal broadening as a result of the formation of a gel. Furthermore, the solvent dependency of the number of peaks and chemical shifts is clearly shown (see Figure 2E and F, four peaks in the range between 39 and 43 ppm related to $2\times CH_2NHCO$ and $2\times CH_2NH_2$ carbon atoms in $CDCl_3$, and Figure 2D, three peaks resulting from the same carbon atoms in the $CDCl_3$/CD_3OD mixture). The last observation also applies to the carbonyl region of the spectrum (Figure 2A–C); two signals, which correspond to three carbonyl carbon atoms, appeared in $CDCl_3$, whereas six signals appeared in the $CDCl_3$/CD_3OD mixture for the same carbonyl atoms. The reason for this behaviour is the coexistent presence and absence of hydrogen bonds between the carbonyl functions and the solvent methanol.[27] This behaviour makes the interpretation of spectra quite demanding and further complicates the comparability of spectra of different lipids. Hence, the choice of NMR solvent is a compromise between solubility and comparability.

Differential scanning calorimetry: The influence of alkyl chain and head group variations on the temperature-dependent aggregation behaviour of aqueous dispersions of the lipids synthesised in this work was investigated to extend the lipid characterisation. For this purpose, we used DSC measurements to examine possible phase transitions. We are aware that our substances are diastereomers and account for this in the analysis of the DSC curves.

The DSC investigations were carried out at two different pH values. At first pH 5 was used to achieve full protonation of the amino groups leading to cationic lipids applicable for gene transfer studies. At this pH value, the lipids form a transparent suspension, which is an indication of the formation of micellar aggregates. In acetate buffer at pH 5, the DSC curves of dispersions of **lipids 1–6c** and **lipids 2,4a** show no transition between 2 and 95 °C (see the Supporting Information). DLS data and TEM images reveal the formation of micelles (data not shown).

Secondly, pH 10 was used for DSC measurements. At this pH value the lipids form a turbid suspension, which is a first indicator for the formation of lamellar or vesicular aggregates (see the Supporting Information for TEM images). Figure 3 summarises the DSC heating curves obtained for aqueous suspensions of all 18 lipids. The DSC scans were performed in a temperature range between 2 and 95 °C in carbonate buffer at pH 10. We chose the alkaline conditions to ensure deprotonation of the amino groups. X-ray scattering data show that **lipids 1–4a–c** build up lamellar phases at

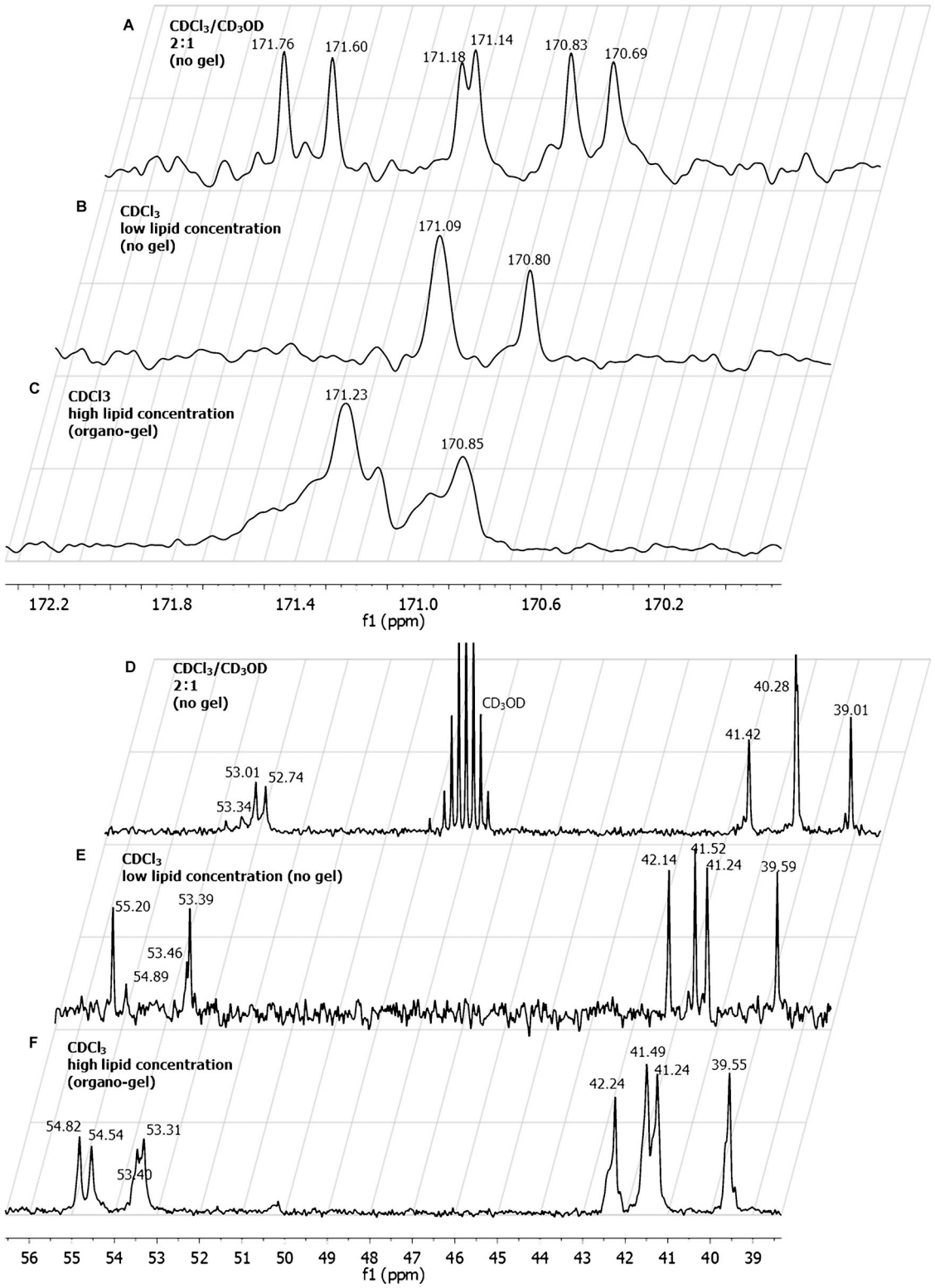

Figure 2. Details of the ^{13}C NMR spectrum of **lipid 1c** measured in different solvents and at different concentrations. A–C) Carbonyl region between 170.0 and 172.3 ppm; D–F) methylene carbon atoms next to amide nitrogen atoms and carbon atoms next to amine moieties in the region between 38 and 56 ppm. A,D) Lipid dissolved in $CDCl_3/CD_3OD$ (2:1, v/v); B,E) lipid dissolved in $CDCl_3$ at low concentration; C,F) lipid dissolved in $CDCl_3$ at high concentration forming an organo-gel.

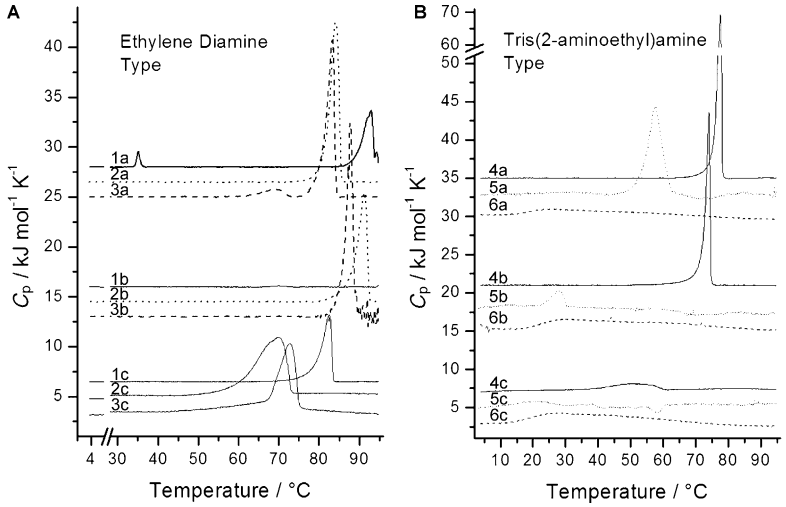

Figure 3. DSC heating curves of aqueous dispersions of the lipids ($c = 1$ mg mL^{-1} in carbonate buffer 10 mM at pH 10). A) Lipids with a head group of the ethylenediamine type (**lipids 1–3a–c**); B) lipids with a head group of the tris(2-aminoethyl)amine type (**lipids 4–6a–c**). The heating rate was 60 K h^{-1}, except for **lipids 5a–c**, which were measured with a heating rate of 20 K h^{-1}. Curves are shifted vertically for clarity.

this pH value.[28] The broadening of the phase transition peaks for lipids with an oleyl chain (OT; see Figure 1) was expected because the oleylamine used contains up to 30% of other alkyl amines with different chain length and saturation.[11b]

The peak maxima (main transition temperature, T_m) of the main endothermic transition peaks and the corresponding enthalpies (ΔH) for the **lipids 1–6a–c** are summarised in Table 1. Other DSC peaks, which appear at lower temperatures than the main DSC peak, are termed herein as pretransitions (T_p as peak maximum). First, we compare the transition temperatures of **lipids 1–3a–c**, which include an ethylenediamine-containing head group, to determine the dependence of the variation in the alkyl chain (Figure 3A). For the smallest lipid head group (**lipids 1a–c**), the main transition temperature increases from **lipid 1a** (92.9 °C) to **lipid 1b** (> 95 °C) due to the longer alkyl chain that is bound to the malonic acid moiety (TT versus TH). In contrast, an unsaturated alkyl chain as residue R^1 (**lipid 1c**, see Figure 1) decreases the transition temperature to 82.5 °C. A similar effect of changes in chain structure on the thermotropic behaviour was observed for the **lipids 2a–c**, including a larger head group with one additional lysine residue and also for the **lipids 3a–c** consisting of two lysine moieties in the head group. The main transition temperatures follow the sequence: T_m(**lipid 2,3b**) > T_m(**lipid 2,3a**) > T_m(**lipid 2,3c**). If we compare the T_m values of lipids with different head groups, while keeping the alkyl chains constant, we see that for all three alkyl-chain combinations (TT, TH, OT) the main transition temperature decreases by roughly 10 K after the insertion of the first lysine moiety and then stays nearly constant after the addition of the second lysine residue to the head group.

The DSC curves of **lipids 4–6a–c**, which contain a tris(2-aminoethyl)amine structure in the head group, differ from those for the **lipids 1–3a–c** described above (Figure 3B). On examining the dependence of T_m on the chain variation of the **lipids 4a–c** and **lipids 5a–c**, both the exchange of a tetradecyl chain by a hexadecyl chain and by an oleyl chain results in a decrease of the main transition temperature for **lipid 4** [T_m(**lipid 4a**) > T_m(**lipid 4b**) > T_m(**lipid 4c**)], as well as for **lipid 5** [T_m(**lipid 5a**) > T_m(**lipid 5b**)]. The dependence of T_m on the head group is similar to that observed for the **lipids 1–3a–c**. The introduction of two additional lysine residues decreases the main transition temperature [T_m(**lipid 4a,b**) > T_m(**lipid 5a,b**)].

Table 1. Main transition temperatures (T_m) and corresponding transition enthalpies (ΔH) of the DSC measurements (heating rate of 60 K h^{-1}) of the lipids.

Lipid	Alkyl chains[a]	Head group Type	Number of lysines	Number of primary amino groups	T_p [°C] (ΔH [kJmol^{-1}])	T_m [°C] (ΔH [kJmol^{-1}])
1a	TT	ethylenediamine	1	2	35.1 (1.7)	92.9 (20.0)
2a			2	3	–	84.2 (47.9)
3a			3	4	69.4 (2.8)	83.4 842.4)
1b	TH		1	2	69.9 (0.6)	–[b]
2b			2	3	–	91.4 (41.3)
3b			3	4	–	86.9 (43.7)
1c	OT		1	2	–	82.5 (24.2)
2c			2	3	–	70.0 (51.7)
3c			3	4	–	72.7 (29.8)
4a	TT	tris(2-aminoethyl)amine	1	3	–	77.6 (52.9)
5a			3	5	–	57.4 (59.1)[c]
6a			4	6	–	–
4b	TH		1	3	–	74.1 (44.1)
5b			3	5	–	27.6 (9.2)[c]
6b			4	6	–	–
4c	OT		1	3	–	60.0 (11.8)
5c			3	5	–[d]	–[d]
6c			4	6	–	–

[a] TT = tetradecyl-/tetradecyl-; TH = tetradecyl-/hexadecyl-; OT = oleyl-/tetradecyl-. [b] The main transition appears at the end of the observed temperature range and could not be determined. [c] The heating rate was 20 K h^{-1}. [d] Data could not be determined because of irreproducible DSC curves.

The **lipids 5a** and **5b** only show reproducible DSC curves at a heating rate of $20\,K\,h^{-1}$. If we used a heating rate of $60\,K\,h^{-1}$, we observed an irreproducible, slow decrease of the heat capacity, C_p, over a wide temperature range, followed by a rapid increase of C_p (see, for example, **lipid 5a** in the Supporting Information). The **lipid 5c** shows no reproducible DSC curves at either heating rate (see the Supporting Information). The DSC curves of **lipids 6a–c** show no transition between 2 and 95 °C, in either the heating or in the cooling scans. This probably indicates that no lamellar phases are formed if the head group becomes too large.

The T_m values of the series of lipids (see Table 1) show clear structure dependence. As mentioned for the class of lipids with an ethylenediamine-containing head group (**lipids 1–3a–c**), we found the following relationships for the lipids with equal head groups: based on the lipids with two tetradecyl chains (TT), the elongation of the malonic acid bound alkyl chain to a hexadecyl chain increases T_m and, on the other hand, the exchange of the lysine-bound alkyl chain by an oleyl chain decreases the main transition temperature. In contrast, the **lipids 4a–c** and **lipids 5a–c** (with tris(2-aminoethyl)amine-containing head groups) show for both alkyl chain variations (TT→TH and TT→OT) a decrease in T_m. The decrease of T_m after the introduction of an oleyl chain is in line with results found for phospholipids; for example, *cis* double bonds reduce the effective alkyl chain length and disturb the chain packing that results in a decrease of T_m.[29] For the exchange of one tetradecyl chain by a hexadecyl chain we would expect an increase of T_m based on principles found for phospholipids.[29] However, only the lipids of the ethylenediamine type show the expected T_m dependencies (T_m(TH) > T_m(TT)). The lipids of the tris(2-aminoethyl)-amine type exhibit the opposite behaviour (T_m(TT) > T_m(TH)). We cannot explain this different behaviour at the moment, but assume a head-group-dependent difference in the molecular conformation, resulting in different packing properties and, as a consequence, deviations from the expected variations of T_m with alkyl-chain length. Further physicochemical investigations such as X-ray scattering are necessary to prove this assumption.

As mentioned before, the attachment of one or two lysine residues to the head group decreases the transition temperature of the **lipids 1–5a–c** on comparing the lipids with the same alkyl chain combination. The **lipids 1a–c** exhibit the smallest head group (see Figure 1), resulting in a cylindrical lipid shape: a structure that allows dense packing of the lipids. The attachment of a lysine molecule to the head group increases the conical shape of the lipids by enlarging the head group. This leads to a decrease of T_m due to a distortion of the lipid packing. Furthermore, we assume a better head-group hydration because of the hydrophilic lysine moieties. This hydration is associated with changes in the properties of the bilayer/solute interface and, hence, also influences the transition temperature.[30] Moreover, the attachment of two lysine residues at the tris(2-aminoethyl)amine head group results in a more conical lipid shape, which explains the observed decrease of the T_m value [T_m(**lipids 4a–c**) > T_m(**lipids 5a–c**)]. The transition temperatures of the **lipids 1–4a–c** present a further head-group effect: all T_m values are equal to or higher than 60 °C. These values are very high taking into account the presence of tetradecyl and oleyl chains. The comparison of the T_m values of **lipids 1–4a–c** with values from glycerol-based phospholipids or cationic lipids containing the same alkyl-chain combination (see data from the literature[31] in Table 2) clearly illustrates the significantly higher transition temperatures. In addition, a group of amino acid based cationic lipids with lysine as head group, two tetradecyl chains as the lipophilic part of the molecule and glutamate as the backbone show lower transition temperatures (T_m between 25.5 and 41.0 °C) than the **lipids 1–4a**.[32] This observation indicates a very strong hydrogen-bonding interaction between the head group and/or lipid-backbone region in addition to the van der Waals interaction between the alkyl chains.[30,33] Another piece of evidence that supports this assumption is the high transition enthalpy of the main transition of **lipids 2–5a** (42.4–59.1 $kJ\,mol^{-1}$; see Table 1). These values exceed the range of the L_α/L_β phase transition enthalpies of 1,2-diacyl-*sn*-glycero-3-phospholipids and glycolipid bilayers of comparable hydrocarbon-chain length (published ΔH values ≈21–25 $kJ\,mol^{-1}$).[31c] Furthermore, high enthalpy values are also observed for **lipids 2b**, **3b**, **4b** and **2c** (see Table 1). The enthalpy change that occurs during a transition in lamellar phases is caused by conformational changes within the lipid hydrocarbon chains, by changes in van der Waals interactions due to an increase in the molecular area at the bilayer/water interface, and also by contributions from the changes in heat of hydration of the head group and the breaking of hydrogen bonds in the backbone and/or head-group region. At present, we have no clear evidence for the assumption of better chain packing and additional hydrogen-bonding interactions in the head-group region. Additional experiments in-

Table 2. Main transition temperature (T_m) values from glycerol-based phospholipids or cationic lipids in different media taken from the literature.

Lipid[a]	Medium	T_m [°C] (ΔH [$kJ\,mol^{-1}$])
DMPC	H_2O, pH 7	24.0
DMPC	H_2O, pH 12	23.6
DMPE	H_2O, pH 7	51.3
DMPE	H_2O, pH 12	21.5
DMTAP	Na_2HPO_4 (50 mM), NaH_2PO_4, pH 7.4	38.4
MPPC	H_2O	34.0 (33.8)
PMPC	H_2O	26.0 (32.6)
MOPC	H_2O, ethylene glycol	−19.0 (20.1)
OMPC	H_2O, ethylene glycol	−27.0

[a] DMPC = 1,2-dimyristoyl-*sn*-glycero-3-phosphocholine, DMPE = 1,2-dimyristoyl-*sn*-glycero-3-phosphoethanolamine, DMTAP = 1,2-dimyristoyl-3-trimethylammonio propane chloride, MPPC = 1-myristoyl-2-palmitoyl-*sn*-glycero-3-phosphocholine, PMPC = 1-palmitoyl-2-myristoyl-*sn*-glycero-3-phosphocholine, MOPC = 1-myristoyl-2-oleoyl-*sn*-glycero-3-phosphocholine, OMPC = 1-oleoyl-2-myristoyl-*sn*-glycero-3-phosphocholine.

cluding X-ray diffraction and infrared spectroscopy are necessary to prove this notion.

Comparing the lipid structures of **lipids 6a–c**, they only vary in the length and degree of saturation of the alkyl chains (see Figure 1). These lipids show no transitions in the DSC scans, presumably due to the formation of micellar aggregates. Based on the chemical structure (Figure 1), we can assume two explanations for the absence of transition peaks in the DSC curves: 1) lipids with six primary amino groups are very hydrophilic and, hence, soluble in carbonate buffer at pH 10; and 2) the lipids self-assemble into micelle-like aggregates that do not show endothermic transitions. To obtain further information about the shape and size of the aggregates of **lipids 6a–c** formed in aqueous dispersions, we investigated the aggregate size by using DLS and visualised the aggregates with TEM.

Particle size measurements: The results of the DLS measurements (intensity and mass-weighted radii of the particles) are summarised in Table 3. Besides the intensity-weighted particle size, we also used the mass-weighted particle size distribution because this is more meaningful for polydisperse samples with different particle species.[34] All investigated lipids reproducibly showed two species of particles with different radii in aqueous dispersions (carbonate buffer at pH 10, $c = 1\,\mathrm{mg\,mL^{-1}}$). This observation refutes the theory that the **lipids 6a–c** are molecularly dissolved in aqueous media. The dominant species has a particle size (radius) of between 4 and 6 nm for all investigated lipid dispersions. This particle size indicates that aggregates of a micellar type are probably present in the aqueous suspension. The theoretical length of the lipid molecules, which is in the range between 2.5 and 3.0 nm (see the Supporting Information), supports this hypothesis. Under the assumption that the radius of a micelle equals approximately the length of one lipid molecule and bearing in mind that DLS determines the hydrodynamic radius, the radii determined by DLS measurements are in line with the theoretical values. Another supporting fact is the shape of our lipid molecules: the large hydrophilic head group of **lipids 6a–c** with three lysine molecules within the head group causes a distinct conical shape, which prefers the formation of micelles.[35] Furthermore, a second species of aggregate with a larger radius (about 1–2 % of all aggregates in the mass-weighted particle size distribution) was observed (see Table 3). These aggregates, with radii in the range between 35 and 155 nm, are too large for micellar structures. It is conceivable that these aggregates are agglomerates of micelles. To visualise the shape of the aggregates, TEM investigations were performed.

Table 3. Particle sizes of aggregates formed of **lipids 6a–c** ($c = 1\,\mathrm{mg\,mL^{-1}}$, in carbonate buffer at pH 10).

Lipid	Peak 1 r [nm] area [%])[a]	Peak 2 r [nm] (area [%])[a]
intensity weighted:		
lipid 6a	4.4 ± 0.1 (22.2 ± 1.7)	196.2 ± 160.3 (68.8 ± 14.4)
lipid 6b	4.4 ± 0.1 (17.9 ± 0.6)	46.9 ± 2.1 (76.1 ± 4.5)
lipid 6c	6.1 ± 0.2 (10.7 ± 0.5)	85.9 ± 1.3 (85.7 ± 1.4)
mass weighted:		
lipid 6a	3.8 ± 0.3 (99.1 ± 0.3)	155.6 ± 76.2 (0.9 ± 0.3)
lipid 6b	4.1 ± 0.2 (99.2 ± 0.1)	34.6 ± 2.8 (0.7 ± 0.1)
lipid 6c	5.4 ± 0.2 (97.7 ± 0.1)	95.6 ± 3.6 (2.2 ± 0.1)

[a] The averages of the particle radii and the corresponding peak areas are given with the corresponding standard deviations ($n = 3$).

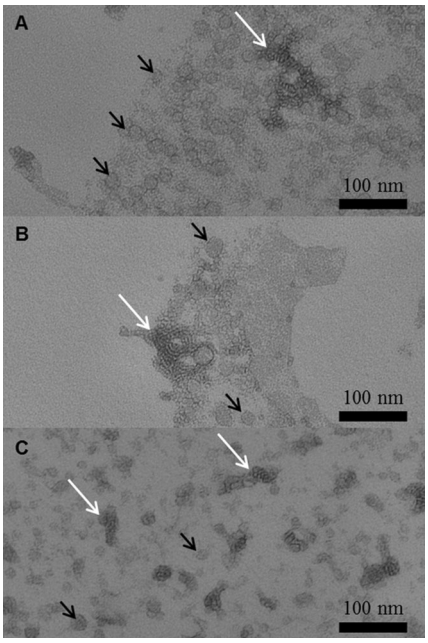

Figure 4. TEM images of lipid dispersions ($c = 0.05\,\mathrm{mg\,mL^{-1}}$ in carbonate buffer at pH 10): A) **lipid 6a**; B) **lipid 6b**; C) **lipid 6c**. The samples were stained with uranyl acetate. Black arrows point to small round aggregates (micelles). White arrows point to larger agglomerates.

Transmission electron microscopy: Figure 4 shows TEM images of lipid dispersions containing $0.05\,\mathrm{mg\,mL^{-1}}$ of lipid (**lipids 6a–c**, Figure 4 A–C, respectively) in carbonate buffer at pH 10. The samples were negatively stained with uranyl acetate. All three images show two species of aggregates with different particle sizes that are roughly in agreement with the DLS results mentioned above. We observed nearly round aggregates with radii of about 10 nm (see Figure 4, black arrows) and some larger agglomerates, which consist of small spherical aggregates (micelles) with radii smaller than 4 nm (see Figure 4, white arrows). These observations are in agreement with the micelle hypothesis proposed above for aqueous dispersions of **lipids 6a–c**.

Conclusion

A new structure type of amino-functionalised lipids has been synthesised. These lipids exhibit a complex malonic

acid diamide backbone and represent the second generation of the malonic acid diamides. The lipids contain six head-group types of variable size and different numbers of amino moieties, as well as three different types of alkyl chain. The use of lysine as a major component of the lipids and the high number of amide bonds determine the peptide-mimic character of the lipids. The modular nature of the synthesis of the lipid backbone, as well as the head-group attachment, results in a wide variation in the lipid structures. The combination of different alkyl chains with head groups of variable size and number of amino groups allow a detailed investigation of structure dependencies for subsequent research activities.

Head-group dependent and alkyl-chain dependent influences on the main transition temperatures of the **lipids 1–5a–c** at pH 10 were found: the introduction of lysine in the head group decreases the T_m value. The alkyl-chain effect was different between lipids of the ethylenediamine type (T_m(TH) > T_m(TT) > T_m(OT)) and tris(2-aminoethyl)amine type (T_m(TT) > T_m(TH) > T_m(OT)). The observed high transition temperature and enthalpy values indicate strong interactions in the head group and backbone region. This assumption is supported by observations from NMR measurements.

Special thermal behaviour was observed for **lipids 6**, bearing the largest head group with six primary amino moieties. These lipids exhibit no phase transition in the observed temperature region. DLS and TEM investigations indicate that these lipids form micellar aggregates in an aqueous environment. The micelles tend to agglomerate, resulting in the formation of larger aggregates.

First results suggest that the gene-transfer efficiencies of these lipids are very promising. Further physicochemical investigations with respect to the complexation ability of polynucleotides (as pure lipid or in a mixture with other lipids), including other scattering techniques and transfection experiments to test the transfection efficiency of the amino-functionalised lipids, are currently under way.

Experimental Section

General: All materials and reagents were purchased from Sigma Aldrich Co. Ltd. unless stated otherwise. All solvents were analytically pure and dried before use. Thin-layer chromatography was carried out on aluminium sheets pre-coated with silica gel 60 F254 (Merck, Darmstadt) and developed with bromothymol blue dip. For column chromatography under normal pressure, silica gel 60 (0.063–0.200 mm) was used. Mass spectrometry analyses were performed with a Finnigan MAT 710C instrument (Thermoseparation Products, San Jose, CA) for ESI-MS, and with an LTQ Orbitrap mass spectrometer (Thermo Fisher Scientific, Bremen) for HRMS. ^{1}H and ^{13}C NMR spectra were recorded on Varian Gemini 2000 and Varian Inova 500 instruments. In general, we used $CDCl_3$ for ^{1}H NMR spectroscopy and a $CDCl_3$/CD_3OD mixture (2:1, v/v) for ^{13}C NMR spectroscopy. In some cases, we had to vary the solvent composition and the solvent (by using D_2O) due to solubility problems. Elemental analyses were performed with a CHNS-932 apparatus (Leco Corporation, St. Joseph, MI). MilliQ water was produced with a Milli-Q Advantage A10 pure-water system (Millipore, Billerica, MA).

Lipid precursor synthesis: The synthesis of the monoalkylated malonic acid diethyl esters (**5a** and **b**) and monoethyl esters (**6a** and **b**) was described previously.[10a,17a,b,f]

Synthesis of orthogonally protected alkyl lysine amides (2a and **b)**: Tetradecylamine or oleylamine (10 mmol) and DIPEA (10 mmol, 1.29 g) were dissolved in CH_2Cl_2 (10 mL). A solution of Fmoc-Lys(Boc)-OH (**1**; 10 mmol, 4.69 g) and PyBOP (10 mmol, 5.20 g) in CH_2Cl_2 (50 mL) was added under an argon atmosphere whilst stirring, which was continued for 3 h at room temperature. Afterwards, the reaction mixture was diluted with $CHCl_3$ and washed with saturated aqueous $NaHCO_3$. The organic layer was washed with brine, dried over Na_2SO_4, filtered and the solvent was evaporated in vacuo. The crude compounds **2a** and **b** were purified by column chromatography using silica gel 60 and $CHCl_3$/MeOH with the gradient technique.

*(2*S*)-6-[(*tert*-Butoxycarbonyl)]amino-2-[(9*H*-fluoren-9-yl)methoxycarbonyl]amino*-N-*tetradecylhexanamide (**2a**)*, $C_{40}H_{61}N_3O_5$: Yield: 82%; R_f = 0.81 ($CHCl_3$/MeOH, 9:1, v/v); m.p. 129–132°C; ^{1}H NMR (500 MHz, $CDCl_3$, 27°C): δ = 0.88 (t, ^3J(H,H) = 7.0 Hz, 3H; CH_2CH_3), 1.23–1.84 (m, 39H; $CH_2(CH_2)_{12}CH_3$, $(CH_2)_3CH_2$NHBoc, OC$(CH_3)_3$), 3.09–3.22 (m, 4H; CH_2NHCO, CH_2NHBoc), 4.10–4.11 (m, 1H; COC*H*NHFmocCH_2), 4.20 (t, ^3J(H,H) = 7.0 Hz, 1H; *H*9-fluorene), 4.38–4.39 (m, 2H; CH_2-fluorene), 4.63 (s, 1H; N*H*Boc), 5.58 (s, 1H; N*H*Fmoc), 6.20 (s, 1H; N*H*CO), 7.30 (t, ^3J(H,H) = 7.5 Hz, 2H; *H*3,*H*6-fluorene), 7.39 (t, ^3J(H,H) = 7.5 Hz, 2H; *H*2,*H*7-fluorene), 7.58 (d, ^3J(H,H) = 7.4 Hz, 2H; *H*1,*H*8-fluorene); 7.75 ppm (d, ^3J(H,H) = 7.5 Hz, 2H; *H*4,*H*5-fluorene); MS: *m*/*z*: 686 [*M*+Na]$^+$; elemental analysis calcd (%) for $C_{40}H_{61}N_3O_5$: C 72.36, H 9.26, N 6.33; found: C 72.43, H 9.33, N 6.33.

*(2*S*)-6-[(*tert*-Butoxycarbonyl)]amino-2-[(9*H*-fluoren-9-yl)methoxycarbonyl]amino*-N-*[(9*Z*)-octadec-9-enyl]hexanamide (**2b**)*, $C_{44}H_{67}N_3O_5$: Yield: 72%; R_f = 0.72 ($CHCl_3$/MeOH, 9:1, v/v); m.p. 115–116°C; ^{1}H NMR (500 MHz, $CDCl_3$, 27°C): δ = 0.88 (t, ^3J(H,H) = 6.7 Hz, 3H; CH_2CH_3), 1.27–1.86 (m, 39H; $CH_2(CH_2)_6CH_2$CH=CH$CH_2(CH_2)_6CH_3$, $(CH_2)_3CH_2$NHBoc, OC$(CH_3)_3$), 1.96–2.01 (m, 4H; CH_2CH=CHCH_2), 3.10–3.23 (m, 4H; CH_2NHCO, CH_2NHBoc), 4.09–4.10 (m, 1H; COC*H*NHFmocCH_2), 4.20 (t, ^3J(H,H) = 6.9 Hz, 1H; *H*9-fluorene), 4.38–4.40 (m, 2H; CH_2-fluorene), 4.60 (s, 1H; N*H*Boc), 5.33–5.38 (m, 2H; C*H*=C*H*), 5.54 (s, 1H; N*H*Fmoc), 6.14 (s, 1H; N*H*CO), 7.30 (t, ^3J-(H,H) = 7.4 Hz, 2H; *H*3,*H*6-fluorene), 7.39 (t, ^3J(H,H) = 7.4 Hz, 2H; *H*2,*H*7-fluorene), 7.58 (d, ^3J(H,H) = 7.4 Hz, 2H; *H*1,*H*8-fluorene), 7.76 ppm (d, ^3J(H,H) = 7.5 Hz, 2H; *H*4,*H*5-fluorene); MS: *m*/*z*: 741 [*M*+Na]$^+$; elemental analysis calcd (%) for $C_{44}H_{67}N_3O_5$: C 73.60, H 9.41, N 5.85; found: C 73.63, H 9.40, N 5.58.

Fmoc cleavage (3a and b): Alkyl lysine amides **2a** and **b** (10 mmol) and piperidine (64.6 mmol, 5.5 g) were dissolved in DMF (55 mL) and stirred for 3 h at room temperature. Afterwards, the reaction batch was diluted with water and extracted three times with heptane. The organic layers were combined, dried over Na_2SO_4, filtered and the solvent was evaporated in vacuo. The crude compounds **3a** and **b** were purified by column chromatography using silica gel 60 and $CHCl_3$/MeOH/NH_3 with the gradient technique.

*(2*S*)-2-Amino-6-[(*tert*-butoxycarbonyl)]amino*-N-*tetradecylhexanamide (**3a**)*, $C_{25}H_{51}N_3O_3$: Yield: 99%; R_f = 0.82 ($CHCl_3$/MeOH/NH_3, 90:10:0.5, v/v/v); m.p. 67–69°C; ^{1}H NMR (500 MHz, $CDCl_3$, 27°C): δ = 0.87 (t, ^3J-(H,H) = 6.9 Hz, 3H; CH_2CH_3), 1.25–1.87 (m, 39H; $CH_2(CH_2)_{12}CH_3$, $(CH_2)_3CH_2$NHBoc, OC$(CH_3)_3$), 3.11–3.12 (m, 2H; CH_2NHBoc), 3.22 (dd, $^3J_1$(H,H) = 13.5, $^3J_2$(H,H) = 6.7 Hz, 2H; CH_2NHCO), 3.33 (dd, $^3J_1$(H,H) = 7.9, $^3J_2$(H,H) = 4.3 Hz, 1H; COC*H*NH_2CH_2), 4.56 (s, 1H; N*H*Boc), 7.25 ppm (s, 1H; N*H*CO); MS: *m*/*z*: 442 [*M*+H]$^+$, 883 [2*M*+H]$^+$, 464 [*M*+Na]$^+$, 905 [2*M*+Na]$^+$; elemental analysis calcd (%) for $C_{25}H_{51}N_3O_3$: C 67.98, H 11.64, N 9.51; found: C 68.24, H 11.45, N 9.38.

*(2*S*)-2-Amino-6-[(*tert*-butoxycarbonyl)]amino*-N-*[(9*Z*)-octadec-9-enyl]-hexanamide (**3b**)*, $C_{29}H_{57}N_3O_3$: Yield: 94%; R_f = 0.54 ($CHCl_3$/MeOH/NH_3, 90:10:0.5, v/v/v); m.p. 37–38°C; ^{1}H NMR (500 MHz, $CDCl_3$, 27°C): δ = 0.86 (t, ^3J(H,H) = 6.8 Hz, 3H; CH_2CH_3), 1.24–1.87 (m, 39H; CH_2-$(CH_2)_6CH_2$CH=CH$CH_2(CH_2)_6CH_3$, $(CH_2)_3CH_2$NHBoc, OC$(CH_3)_3$), 1.95–2.02 (m, 4H; CH_2CH=CHCH_2), 3.10 (dt, $^3J_1$(H,H) = 6.4, $^3J_2$(H,H) = 6.4 Hz, 2H; CH_2NHBoc), 3.21 (dd, $^3J_1$(H,H) = 6.9, $^3J_2$(H,H) = 6.4 Hz, 2H; CH_2NHCO), 3.31 (dd, $^3J_1$(H,H) = 8.0, $^3J_2$(H,H) = 4.4 Hz, 1H;

COC*H*NH_2CH_2), 4.59 (s, 1H; N*H*Boc), 5.31–5.36 (m, 2H; C*H*=C*H*), 7.25 ppm (s, 1H; N*H*CO); MS: *m/z*: 496 $[M+H]^+$, 991 $[2M+H]^+$, 518 $[M+Na]^+$, 1013 $[2M+Na]^+$; elemental analysis calcd (%) for $C_{29}H_{57}N_3O_3$: C 70.25, H 11.59, N 8.48; found: C 70.04, H 11.27, N 8.51.

Coupling of the lipid backbone (7a–c): The appropriate lysine amide **3a** and **b** (1 mmol) and DIPEA (2 mmol, 250.5 mg) were dissolved in CH_2Cl_2 (3 mL). A solution of the appropriate alkyl malonic acid monoethyl ester **6a** and **b** (1 mmol) and PyBOP (1 mmol, 520,4 mg) in CH_2Cl_2 (15 mL) was added under an argon atmosphere whilst stirring, which was continued for 16 h. Afterwards, the reaction mixture was diluted with $CHCl_3$ and washed with aqueous $NaHCO_3$ (5%). Then, the organic layer was washed with brine, dried over Na_2SO_4, filtered and the solvent was evaporated in vacuo. The crude compounds **7a–c** were purified by isocratic column chromatography using silica gel 60 and $CHCl_3/Et_2O$ (1:1, v/v) as eluent.

*2-[(*N*-{6-[(*tert*-Butoxycarbonyl)amino]-1-oxo-1-[(*N*-tetradecyl)amino]hexan-(2*S*)-2-yl}amino)carbonyl]hexadecanoic acid ethyl ester (**7a**), $C_{44}H_{85}N_3O_6$*: Yield: 97%; R_f = 0.47 ($CHCl_3/Et_2O$, 1:1, v/v); m.p. 84–87 °C; ^{1}H NMR (500 MHz, $CDCl_3$, 27 °C): δ = 0.87 (t, ^3J(H,H) = 6.9 Hz, 6H; 2× $(CH_2)_2CH_3$), 1.25–1.92 (m, 68H; $NHCH_2(CH_2)_{12}CH_3$, $(CH_2)_{13}CH_3$, $(CH_2)_3CH_2NHBoc$, OCH_2CH_3, $OC(CH_3)_3$), 3.03–3.14 (m, 2H; CH_2NHBoc), 3.19–3.24 (m, 3H; CH_2NHCO, COC*H*(tetradecyl)CO), 4.15–4.22 (m, 2H; OCH_2CH_3), 4.32–4.37 (m, 1H; COC*H*(NHCO)CH_2), 4.61 (s, 1H; N*H*Boc), 6.26/6.36 (2×s, 1H; CH_2NHCO), 6.91 (^3J(H,H) = 8.0 Hz)/6.96 ppm (^3J(H,H) = 7.7 Hz) (2×d, 1H; COCH(N*H*CO)CH_2); MS: *m/z*: 750 $[M+H]^+$, 774 $[M+Na]^+$, 1526 $[2M+Na]^+$; elemental analysis calcd (%) for $C_{44}H_{85}N_3O_6$: C 70.26, H 11.39, N 5.59; found: C 70.34, H 11.25, N 5.58.

*2-[(*N*-{6-[(*tert*-Butoxycarbonyl)amino]-1-oxo-1-[(*N*-tetradecyl)amino]hexan-(2*S*)-2-yl}amino)carbonyl]octadecanoic acid ethyl ester (**7b**), $C_{46}H_{89}N_3O_6$*: Yield: 96%; R_f = 0.48 ($CHCl_3/Et_2O$, 1:1, v/v); m.p. 87–89 °C; ^{1}H NMR (500 MHz, $CDCl_3$, 27 °C): δ = 0.88 (t, ^3J(H,H) = 6.9 Hz, 6H; 2× $(CH_2)_2CH_3$), 1.25–1.92 (m, 72H; $NHCH_2(CH_2)_{12}CH_3$, $(CH_2)_{15}CH_3$, $(CH_2)_3CH_2NHBoc$, OCH_2CH_3, $OC(CH_3)_3$), 3.03–3.15 (m, 2H; CH_2NHBoc), 3.18–3.24 (m, 3H; CH_2NHCO, COC*H*(hexadecyl)CO), 4.14–4.24 (m, 2H; OCH_2CH_3), 4.32–4.37 (m, 1H; COC*H*(NHCO)CH_2), 4.61 (s, 1H; N*H*Boc), 6.25/6.36 (2×s, 1H; CH_2NHCO), 6.91 (^3J(H,H) = 7.9 Hz)/7.00 ppm (^3J(H,H) = 7.7 Hz) (2×d, 1H; COCH(N*H*CO)CH_2); MS: *m/z*: 802 $[M+Na]^+$, 778 $[M-H]^-$, 814 $[M+Cl]^-$; elemental analysis calcd (%) for $C_{46}H_{89}N_3O_6$: C 70.81, H 11.50, N 5.39; found: C 71.01, H 11.19, N 5.39.

*2-[(*N*-{6-[(*tert*-Butoxycarbonyl)amino]-1-{*N*-[(9*Z*)-octadec-9-enyl]amino}-1-oxohexan-(2*S*)-2-yl}amino)carbonyl]hexadecanoic acid ethyl ester (**7c**), $C_{48}H_{91}N_3O_6$*: Yield: 93%; R_f = 0.44 ($CHCl_3/Et_2O$, 1:1, v/v); m.p. 70–71 °C; ^{1}H NMR (500 MHz, $CDCl_3$, 27 °C): δ = 0.88 (t, ^3J(H,H) = 6.70 Hz, 6H; 2× $(CH_2)_2CH_3$), 1.25–1.92 (m, 68H; $NHCH_2(CH_2)_6CH_2CH{=}CHCH_2$-$(CH_2)_6CH_3$, $(CH_2)_{13}CH_3$, $(CH_2)_3CH_2NHBoc$, OCH_2CH_3, $OC(CH_3)_3$), 1.93–2.05 (m, 4H; $CH_2CH{=}CHCH_2$), 3.02–3.25 (m, 5H; CH_2NHBoc, CH_2NHCO, COC*H*(tetradecyl)CO), 4.15–4.24 (m, 2H; OCH_2CH_3), 4.31–4.38 (m, 1H; COC*H*(NHCO)CH_2), 4.61 (s, 1H; N*H*Boc), 5.32–5.38 (m, 2H; C*H*=C*H*), 6.22/6.36 (2×s, 1H; CH_2NHCO), 6.91 (^3J(H,H) = 7.8 Hz)/6.98 ppm (^3J(H,H) = 7.6 Hz) (2×d, 1H; COCH(N*H*CO)CH_2); MS: *m/z*: 829 $[M+Na]^+$; elemental analysis calcd (%) for $C_{48}H_{91}N_3O_6$: C 71.51, H 11.38, N 5.21; found: C 71.28, H 11.28, N 5.03.

Saponification of 7a–c (8a–c): The appropriate ester **7a–c** (1 mmol) was dissolved in a mixture of THF (15 mL) and water (5 mL), and potassium hydroxide (1.5 mmol, 84.2 mg) was added. The mixture was stirred for 46 h at room temperature. Then, a solution of H_2SO_4 (0.75 mmol, 73.6 mg) in water (13 mL) was added while stirring and cooling with an ice bath. The mixture was stirred for 15 min, followed by extraction with $CHCl_3$. The organic layer was washed with brine, dried over Na_2SO_4, filtered and the solvent was evaporated. The crude compounds **8a–c** were purified by column chromatography using silica gel 60 and $CHCl_3$/MeOH with the gradient technique.

*2-[(*N*-{6-[(*tert*-Butoxycarbonyl)amino]-1-oxo-1-[(*N*-tetradecyl)amino]hexan-(2*S*)-2-yl}amino)carbonyl]hexadecanoic acid (**8a**), $C_{42}H_{81}N_3O_6$*: Yield: 89%; R_f = 0.39 ($CHCl_3$/MeOH, 9:1, v/v); m.p. 107–110 °C; ^{1}H NMR (500 MHz, $CDCl_3$, 27 °C): δ = 0.88 (t, ^3J(H,H) = 6.9 Hz, 6H; 2× CH_2CH_3), 1.25–1.88 (m, 65H; $NHCH_2(CH_2)_{12}CH_3$, $(CH_2)_{13}CH_3$, $(CH_2)_3CH_2NHBoc$, $OC(CH_3)_3$), 3.02–3.26 (m, 5H; CH_2NHBoc, CH_2NHCO, COC*H*(tetradecyl)CO), 4.42–4.43 (m, 1H; COCH(NHCO)RCH_2), 4.73 (s, 1H; N*H*Boc), 6.65–6.83 (m, 1H; N*H*CO), 7.34–7.44 ppm (m, 1H; N*H*CO); MS: *m/z*: 747 $[M+Na]^+$, 1471 $[2M+Na]^+$, 1488 $[2M+K]^+$, 723 $[M-H]^-$, 1446 $[2M-H]^-$; elemental analysis calcd (%) for $C_{42}H_{81}N_3O_6$: C 69.66, H 11.27, N 5.80; found: C 69.36, H 10.99, N 5.78.

*2-[(*N*-{6-[(*tert*-Butoxycarbonyl)amino]-1-oxo-1-[(*N*-tetradecyl)amino]hexan-(2*S*)-2-yl}amino)carbonyl]octadecanoic acid (**8b**), $C_{44}H_{85}N_3O_6$*: Yield: 94%; R_f = 0.30 ($CHCl_3$/MeOH, 9:1 v/v); m.p. 102–105 °C; ^{1}H NMR (500 MHz, $CDCl_3$, 27 °C): δ = 0.88 (t, ^3J(H,H) = 6.8 Hz, 6H; 2× CH_2CH_3), 1.25–1.91 (m, 69H; $NHCH_2(CH_2)_{12}CH_3$, $(CH_2)_{15}CH_3$, $(CH_2)_3CH_2NHBoc$, $OC(CH_3)_3$), 3.03–3.25 (m, 5H; CH_2NHBoc, CH_2NHCO, COC*H*(hexadecyl)CO), 4.37–4.39 (m, 1H; COCH(NHCO)CH_2), 4.70 (s, 1H; N*H*Boc), 6.32–6.41 (m, 1H; N*H*CO), 7.07–7.16 ppm (m, 1H; N*H*CO); MS: *m/z*: 775 $[M+Na]^+$, 1526 $[2M+Na]^+$, 790 $[M+K]^+$, 751 $[M-H]^-$; elemental analysis calcd (%) for $C_{44}H_{85}N_3O_6$: C 70.26, H 11.39, N 5.59; found: C 69.88, H 11.24, N 5.51.

*2-[(*N*-{6-[(*tert*-Butoxycarbonyl)amino]-1-{*N*-[(9*Z*)-octadec-9-enyl]amino}-1-oxohexan-(2*S*)-2-yl}amino)carbonyl]hexadecanoic acid (**8c**), $C_{46}H_{87}N_3O_6$*: Yield: 95%; R_f = 0.33 ($CHCl_3$/MeOH, 9:1, v/v); m.p. 75–78 °C; ^{1}H NMR (500 MHz, $CDCl_3$, 27 °C): δ = 0.88 (t, ^3J(H,H) = 6.7 Hz, 6H; 2× CH_2CH_3), 1.25–1.90 (m, 65H; $NHCH_2(CH_2)_6CH_2CH{=}CHCH_2$-$(CH_2)_6CH_3$, $(CH_2)_{13}CH_3$, $(CH_2)_3CH_2NHBoc$, $OC(CH_3)_3$), 1.94–2.02 (m, 4H; $CH_2CH{=}CHCH_2$), 3.05–3.27 (m, 5H; CH_2NHBoc, CH_2NHCO, COC*H*(tetradecyl)CO), 4.38–4.46 (m, 1H; COCH(NHCO)CH_2), 4.72 (s, 1H; N*H*Boc), 5.33–5.38 (m, 2H; C*H*=C*H*), 6.53–6.63 (m, 1H; N*H*CO), 7.30–7.35 ppm (m, 1H; N*H*CO); MS: *m/z*: 801 $[M+Na]^+$, 777 $[M-H]^-$, 1554 $[2M-H]^-$; elemental analysis calcd (%) for $C_{46}H_{87}N_3O_6$: C 71.00, H 11.27, N 5.40; found: C 70.78, H 11.12, N 5.47.

Coupling with ethylene diamine (9a–c) or tris(2-aminoethyl)amine (13a–c): Ethylene diamine (20 mmol, 1.20 g) or tris(2-aminoethyl)amine (20 mmol, 2.93 g), respectively, and TEA (2 mmol, 202 mg) were dissolved in CH_2Cl_2 (2 mL). A solution of the appropriate acid **8a–c** (1 mmol) and PyBOP (1 mmol, 520.4 mg) in CH_2Cl_2 (50 mL) was added slowly to the reaction mixture under argon atmosphere whilst stirring, which was continued for further 16 h. Afterwards, the dispersion was filtered and the filtrate was diluted with $CHCl_3$ and washed with aqueous K_2CO_3 (15%). The organic layer was washed with brine, dried over Na_2SO_4, filtered, and solvent was evaporated. The crude product was purified by column chromatography using silica gel 60 and $CHCl_3$/MeOH/NH_3 with gradient technique.

Boc-Lys(Boc)-OSu coupling with primary amino groups (11a–c, 12a–c, 15a–c, 16a–c): The appropriate amount of amino-functionalised lipid, Boc-Lys(Boc)-OSu, and TEA were dissolved in CH_2Cl_2 (20 mL) and stirred for 16 h at room temperature. Following, the mixture was diluted with $CHCl_3$ (20 mL) and washed with aqueous K_2CO_3 (15%). The organic layer was separated, washed with brine, dried over Na_2SO_4, and solvent was evaporated. The crude product was purified by column chromatography using silica gel 60 and $CHCl_3$/MeOH with gradient technique. Reactants and stoichiometric ratios for the reaction with regard to the required product: **11a–c**: **9a–c** (0.5 mmol), Boc-Lys(Boc)-OSu (0.5 mmol), TEA (0.5 mmol); **12a–c**: **10a–c** (0.5 mmol), Boc-Lys(Boc)-OSu (1 mmol), TEA (1 mmol); **15a–c**: **13a–c** (0.5 mmol), Boc-Lys(Boc)-OSu (1 mmol), TEA (1 mmol); **16a–c**: **14a–c** (0.5 mmol), Boc-Lys(Boc)-OSu (1.5 mmol), TEA (1.5 mmol).

Removal of the Boc protective group with trifluoroacetic acid (lipids 1a–c, lipids 2a–c, lipids 3a–c, and lipids 4a–c): The appropriate amount of Boc-protected lipid (0.5 mmol) was dissolved in CH_2Cl_2 (10 mL). The required amount of trifluoroacetic acid (**9a–c** 4 mL; **11a–c** 6 mL; **12a–c** 8 mL; **13a–c** 6 mL) was added stepwise while stirring at room temperature. Then, the solvent was evaporated at 25 °C. The residue was dissolved in $CHCl_3$ (20 mL) and ammonia solution (10 mL, 10%) was added dropwise while stirring, with an ice bath. Afterwards, $CHCl_3$ (20 mL) and aqueous K_2CO_3 (10 mL, 10%) were added to the dispersion. The organic layer was separated and the water layer was extracted twice with $CHCl_3$. The combined organic layers were washed with brine, dried over Na_2SO_4 and the solvent was evaporated. The crude product was pu-

rified by column chromatography using silica gel 60 and $CHCl_3$/MeOH/NH_3 with the gradient technique.

N-*(2-Aminoethyl)*-N′-*[6-amino-1-oxo-1-[(*N-tetradecylamino*)hexan-(2*S*)-2-yl]*-2-tetradecylpropandiamide (***lipid 1a***), $C_{39}H_{79}N_5O_3$: Yield: 94%; R_f = 0.36 ($CHCl_3$/MeOH/NH_3, 80:20:2, v/v/v); ^{1}H NMR (500 MHz, $CDCl_3$, 27°C): δ = 0.88 (t, ^3J(H,H) = 6.9 Hz, 6H; 2×CH_3), 1.25–1.88 (m, 56H; $NHCH_2(CH_2)_{12}CH_3$, $(CH_2)_{13}CH_3$, $(CH_2)_3CH_2NH_2$), 2.70 (t, ^3J(H,H) = 6.5 Hz, 2H; $(CH_2)_3CH_2NH_2$), 2.83 (t, ^3J(H,H) = 5.9 Hz, 2H; $NHCH_2CH_2NH_2$), 3.00 (t, ^3J(H,H) = 7.6 Hz, 1H; COC*H*(tetradecyl)CO), 3.18–3.36 (m, 4H; 2×CH_2NHCO), 4.30–4.34 (m, 1H; COC*H*-(NHCO)CH_2), 6.30–6.32 (m, 1H; tetradecyl-N*H*CO), 6.85–6.87 (m, 1H; N*H*$CH_2CH_2NH_2$), 7.16 ppm (d, ^3J(H,H) = 7.9 Hz, 1H; COCH-(N*H*CO)CH_2); ^{13}C NMR (125 MHz, $CDCl_3$, 27°C): δ = 13.7, 22.4, 22.4, 22.5, 26.7, 27.2, 27.27, 27.29, 29.0, 29.07, 29.09, 29.2, 29.3, 29.36, 29.39, 29.41, 29.43, 31.0, 31.31, 31.35, 31.7, 39.3, 40.52, 40.57, 41.60, 41.64, 53.3, 53.2, 53.3, 54.7, 171.0, 171.1, 171.2, 171.3, 171.6, 171.7 ppm; MS: *m*/*z*: 666 $[M+H]^+$, 334 $[M+2H]^{2+}$, 688 $[M+Na]^+$,664 $[M-H]^-$; HRMS calcd for $C_{39}H_{80}N_5O_3$ $[M+H]^+$: 666.6256; found: 666.6255.

N-*(2-Aminoethyl)*-N′-*[6-amino-1-oxo-1-(*N-tetradecylamino*)hexan-(2*S*)-2-yl]*-2-hexadecylpropandiamide (***lipid 1b***), $C_{41}H_{83}N_5O_3$: Yield: 71%; R_f = 0.27 ($CHCl_3$/MeOH/NH_3, 80:20:2, v/v/v); ^{1}H NMR (500 MHz, $CDCl_3$, 27°C): δ = 0.88 (t, ^3J(H,H) = 6.9 Hz, 6H; 2×CH_3), 1.25–1.90 (m, 60H; $NHCH_2(CH_2)_{12}CH_3$, $(CH_2)_{15}CH_3$, $(CH_2)_3CH_2NH_2$), 2.70 (t, ^3J(H,H) = 6.6 Hz, 2H; $(CH_2)_3CH_2NH_2$), 2.82 (t, ^3J(H,H) = 5.9 Hz, 2H; $NHCH_2CH_2NH_2$), 3.01 (t, ^3J(H,H) = 7.7 Hz, 1H; COC*H*(hexadecyl)CO), 3.16–3.35 (m, 4H; 2×CH_2NHCO), 4.28–4.35 (m, 1H; COC*H*-(NHCO)CH_2), 6.33–6.37 (m, 1H; tetradecyl-N*H*CO), 6.87–6.90 (m, 1H; N*H*$CH_2CH_2NH_2$), 7.20 ppm (d, ^3J(H,H) = 7.7 Hz, 1H; COCH-(N*H*CO)CH_2); ^{13}C NMR (125 MHz, $CDCl_3$/CD_3OD, 27°C): δ = 13.7, 22.2, 22.3, 22.42, 26.48, 27.1, 27.1, 28.82, 28.90, 28.93, 29.0, 29.15, 29.17, 29.19, 29.22, 29.24, 30.9, 31.0, 31.15, 31.17, 31.3, 31.5, 39.1, 40.34, 40.39, 40.42, 41.52, 52.8, 53.1, 53.4, 53.8, 170.8, 170.9, 171.2, 171.3, 171.6, 171.8 ppm; MS: *m*/*z*: 694 $[M+H]^+$, 345 $[M+2H]^{2+}$, 728 $[M+Cl]^-$, 693 $[M-H]^-$; HRMS calcd for $C_{41}H_{84}N_5O_3$ $[M+H]^+$: 694.6569; found: 694.6567.

N-*(2-Aminoethyl)*-N′-*[6-amino-1-[*N-*(9*Z*)-octadec-9-enylamino]-1-oxohexan-(2*S*)-2-yl]*-2-tetradecylpropandiamide (***lipid 1c***), $C_{43}H_{85}N_5O_3$: Yield: 92%; R_f = 0.20 ($CHCl_3$/MeOH/NH_3, 80:20:2, v/v/v); ^{1}H NMR (500 MHz, $CDCl_3$, 27°C): δ = 0.88 (t, ^3J(H,H) = 6.9 Hz, 6H; 2×CH_3), 1.24–1.89 (m, 56H; $NHCH_2(CH_2)_6CH_2CH{=}CHCH_2(CH_2)_6CH_3$, $(CH_2)_{13}CH_3$, $(CH_2)_3CH_2NH_2$), 1.95–2.02 (m, 8H; 2×$CH_2CH{=}CHCH_2$), 2.70 (t, ^3J-(H,H) = 6.7 Hz, 2H; $(CH_2)_3CH_2NH_2$), 2.82 (t, ^3J(H,H) = 5.9 Hz, 2H; $NHCH_2CH_2NH_2$), 3.04 (t, ^3J(H,H) = 7.5 Hz, 1H; COC*H*(tetradecyl)CO), 3.14–3.33 (m, 4H; 2×CH_2NHCO), 4.28–4.35 (m, 1H; COC*H*-(NHCO)CH_2), 5.33–5.38 (m, 2H; C*H*=C*H*), 6.45–6.46 (m, 1H; oleyl-N*H*CO), 7.02–7.03 (m, 1H; N*H*$CH_2CH_2NH_2$), 7.33–7.40 ppm (m, 1H; COCH(N*H*CO)CH_2); ^{13}C NMR (125 MHz, $CDCl_3$/CD_3OD, 27°C): δ = 13.4, 22.1, 22.27, 22.35, 26.4, 26.7, 26.98, 27.03, 28.76, 28.83, 28.87, 29.0, 29.1, 29.17, 29.22, 30.1, 30.76, 30.83, 30.99, 31.06, 31.1, 31.2, 31.4, 32.0, 39.0, 40.29, 40.32, 41.4, 52.8, 53.0, 53.3, 129.2, 129.4, 170.7, 170.8, 171.1, 171.2, 171.6, 171.7 ppm; MS: *m*/*z*: 720.5 $[M+H]^+$, 361.1 $[M+2H]^{2+}$, 754.5 $[M+Cl]^-$, 718.6 $[M-H]^-$; HRMS calcd for $C_{43}H_{86}N_5O_3$ $[M+H]^+$: 720.6725; found: 720.6750.

N-*[6-Amino-1-oxo-1-(*N-tetradecylamino*)hexan-(2*S*)-2-yl]*-N′-*[2-(*N-*{(2*S*)-2,6-diamino]-1-oxohexyl}amino)ethyl]*-2-tetradecylpropandiamide (***lipid 2a***), $C_{45}H_{91}N_7O_4$: Yield: 89%; R_f = 0.15 ($CHCl_3$/MeOH/NH_3, 65:35:5, v/v/v); ^{1}H NMR (500 MHz, $CDCl_3$, 27°C): δ = 0.88 (t, ^3J(H,H) = 6.9 Hz, 6H; 2×CH_3), 1.25–1.88 (m, 62H; $NHCH_2(CH_2)_{12}CH_3$, $(CH_2)_{13}CH_3$, 2×$(CH_2)_3CH_2NH_2$), 2.69–2.74 (m, 4H; 2×CH_2NH_2), 2.99 (t, ^3J(H,H) = 7.5 Hz, 1H; COC*H*(tetradecyl)CO), 3.16–3.46 (m, 7H; 3×CH_2NHCO, C*H*NH_2CH_2), 4.26–4.32 (m, 1H; COC*H*(NHCO)CH_2), 6.47–6.49/6.62–6.64/7.56–7.58/7.66–7.74 (4×m, 3H; 3×N*H*CO), 7.20–7.31 ppm (m, 1H; COCH(N*H*CO)CH_2); ^{13}C NMR (125 MHz, $CDCl_3$/CD_3OD, 27°C): δ = 13.5, 22.3, 22.4, 22.5, 26.6, 27.1, 28.89, 28.94, 29.1, 29.20, 29.24, 29.3, 31.2, 31.4, 31.5, 31.8, 32.0, 34.4, 34.5, 38.4, 38.5, 38.6, 38.8, 39.17, 39.20, 40.7, 40.8, 49.2, 52.9, 53.1, 54.5, 54.6, 170.7, 170.8, 171.0, 171.5, 171.6, 171.9, 175.9, 176.0 ppm; MS: *m*/*z*: 794.7 $[M+H]^+$, 398.1 $[M+2H]^{2+}$, 828.5 $[M+Cl]^-$, 792.6 $[M-H]^-$; HRMS calcd for $C_{45}H_{92}N_7O_4$ $[M+H]^+$: 794.7205; found: 794.7208.

N-*[6-Amino-1-oxo-1-(*N-tetradecylamino*)hexan-(2*S*)-2-yl]*-N′-*[2-(*N-*{(2*S*)-2,6-diamino-1-oxohexyl}amino)ethyl]*-2-hexadecylpropandiamide (***lipid 2b***), $C_{47}H_{95}N_7O_4$: Yield: 70%; R_f = 0.18 ($CHCl_3$/MeOH/NH_3, 65:35:5, v/v/v); ^{1}H NMR (500 MHz, $CDCl_3$, 27°C): δ = 0.88 (t, ^3J(H,H) = 6.9 Hz, 6H; 2×CH_3), 1.25–1.88 (m, 66H; $NHCH_2(CH_2)_{12}CH_3$, $(CH_2)_{15}CH_3$, 2×$(CH_2)_3CH_2NH_2$), 2.69–2.74 (m, 4H; 2×CH_2NH_2), 2.99 (t, ^3J(H,H) = 7.5 Hz, 1H; COC*H*(hexadecyl)CO), 3.16–3.46 (m, 7H; 3×CH_2NHCO, C*H*NH_2CH_2), 4.26–4.32 (m, 1H; COC*H*(NHCO)CH_2), 6.47–6.49/6.62–6.64/7.56–7.58/7.66–7.74 (4×m, 3H; 3×N*H*CO), 7.20–7.31 ppm (m, 1H; COCH(N*H*CO)CH_2); ^{13}C NMR (125 MHz, $CDCl_3$/CD_3OD, 27°C): δ = 13.7, 22.1, 22.3, 22.4, 26.7, 27.2, 29.0, 29.09, 29.19, 29.26, 29.36, 29.40, 29.45, 29.6, 29.7, 30.6, 31.19, 31.29, 31.7, 34.24, 38.57, 38.68, 38.78, 38.82, 39.3, 39.4, 40.02, 40.08, 49.5, 53.1, 53.2, 54.35, 54.40, 170.82, 170.87, 171.0, 171.3, 171.9, 172.0, 175.9, 176.0 ppm; MS: *m*/*z*: 822.6 $[M+H]^+$, 844.7 $[M+Na]^+$, 856.6 $[M+Cl]^-$, 820.6 $[M-H]^-$; HRMS calcd for $C_{47}H_{96}N_7O_4$ $[M+H]^+$: 822.7518; found: 822.7518.

N-*[6-Amino-1-[*N-*(9*Z*)-octadec-9-enylamino]-1-oxohexan-(2*S*)-2-yl]*-N′-*[2-(*N-*{(2*S*)-2,6-diamino-1-oxohexyl}amino)ethyl]*-2-tetradecylpropandiamide (***lipid 2c***), $C_{49}H_{97}N_7O_4$: Yield: 81%; R_f = 0.09 ($CHCl_3$/MeOH/NH_3 65:35:5, v/v/v); ^{1}H NMR (500 MHz, $CDCl_3$, 27°C): δ = 0.88 (t, ^3J(H,H) = 6.9 Hz, 6H; 2×CH_3), 1.23–1.86 (m, 62H; $NHCH_2(CH_2)_6CH_2CH{=}CHCH_2(CH_2)_6CH_3$, $(CH_2)_{13}CH_3$, 2×$(CH_2)_3CH_2NH_2$), 1.95–2.02 (m, 4H; $CH_2CH{=}CHCH_2$), 2.69–2.74 (m, 4H; 2×CH_2NH_2), 3.01 (t, ^3J(H,H) = 7.4 Hz, 1H; COC*H*(tetradecyl)CO), 3.13–3.46 (m, 7H; 3×CH_2NHCO, C*H*NH_2CH_2), 4.27–4.32 (m, 1H; COC*H*(NHCO)CH_2), 5.33–5.38 (m, 2H; C*H*=C*H*), 6.58–6.60/7.62–7.63/7.73–7.75 (3×m, 3H; 3×N*H*CO), 7.29–7.30 ppm (m, 1H; COCH(N*H*CO)CH_2); ^{13}C NMR (125 MHz, $CDCl_3$/CD_3OD, 27°C): δ = 13.7, 22.4, 26.7, 26.9, 27.2, 29.1, 29.2, 29.4, 31.25, 31.32, 31.57, 31.64, 31.8, 32.1, 32.3, 34.6, 38.5, 38.6, 38.8, 39.0, 39.3, 39.4, 40.8, 40.9, 53.1, 53.2, 53.7, 54.0, 54.7, 129.4, 129.7, 170.8, 171.0, 171.2, 171.4, 171.6, 171.8, 176.0, 176.2 ppm; MS: *m*/*z*: 848.6 $[M+H]^+$, 425.0 $[M+2H]^{2+}$, 882.6 $[M+Cl]^-$, 846.7 $[M-H]^-$; HRMS calcd for $C_{49}H_{98}N_7O_4$ $[M+H]^+$: 848.7675; found: 848.7671.

N-*[2-(*N-*{(2*S*)-2,6-Diamino-1-oxohexyl}amino)ethyl]*-N′-*[6-(*N-*{(2*S*)-2,6-diamino-1-oxohexyl}amino-1-oxo-1-(*N-tetradecylamino*)hexan-(2*S*)-yl]*-2-tetradecylpropandiamide (***lipid 3a***), $C_{51}H_{103}N_9O_5$: Yield: 31%; R_f = 0.24 ($CHCl_3$/MeOH/NH_3, 50:50:10, v/v/v); ^{1}H NMR (500 MHz, $CDCl_3$, 27°C): δ = 0.88 (t, ^3J(H,H) = 7.0 Hz, 6H; 2×CH_3), 1.24–1.86 (m, 68H; $NHCH_2$-$(CH_2)_{12}CH_3$, $(CH_2)_{13}CH_3$, 2×$(CH_2)_3CH_2NH_2$, $(CH_2)_3CH_2NHCO$), 2.64–2.69 (m, 4H; 2×CH_2NH_2), 3.02–3.07 (m, 1H; COC*H*(tetradecyl)CO), 3.18–3.49 (m, 10H; 4×CH_2NHCO, 2×C*H*NH_2CH_2), 4.27–4.31 (m, 1H; COC*H*(NHCO)CH_2), 6.62–6.64/7.40–7.50/7.62–7.64/7.71–7.73 (4×m, 4H; 4×N*H*CO), 7.34–7.36 ppm (d, ^3J(H,H) = 7.8 Hz, 1H; COCH-(N*H*CO)CH_2); ^{13}C NMR (125 MHz, $CDCl_3$/CD_3OD, 27°C): δ = 12.8, 21.8, 22.03, 22.08, 22.09, 22.2, 22.3, 26.14, 26.15, 26.69, 26.70, 27.96, 28.07, 28.48, 28.50, 28.54, 28.56, 28.61, 28.69, 28.81, 28.84, 28.88, 29.28, 30.37, 30.7, 30.8, 30.9, 31.0, 31.1, 34.0, 34.08, 34.17, 34.20, 37.96, 38.02, 38.07, 38.3, 38.4, 38.71, 38.76, 40.06, 40.13, 40.14, 40.16, 52.7, 52.8, 54.1, 54.2, 170.36, 170.40, 170.8, 171.6, 171.7, 171.8, 175.5, 175.9, 176.0 ppm; MS: *m*/*z*: 922.5 $[M+H]^+$, 461.9 $[M+2H]^{2+}$, 944.6 $[M+Na]^+$, 956.5 $[M+Cl]^-$, 920.5 $[M-H]^-$; HRMS calcd for $C_{51}H_{104}N_9O_5$ $[M+H]^+$: 922.8155; found: 922.8152.

N-*(2-[*N-*{(2*S*)-2,6-Diamino-1-oxohexyl]amino}ethyl)*-N′-*[(2*S*)-2,6-diamino-1-oxo-1-(*N-tetradecylamino*)hexan-(2*S*)-2-yl]*-2-hexadecylpropandiamide (***lipid 3b***), $C_{53}H_{107}N_9O_5$: Yield: 95%; R_f = 0.26 ($CHCl_3$/MeOH/NH_3, 50:50:10, v/v/v); ^{1}H NMR (400 MHz, $CDCl_3$/CD_3OD, 27°C): δ = 0.85 (t, ^3J(H,H) = 6.8 Hz, 6H; 2×CH_3), 1.24–1.96 (m, 68H; $NHCH_2$-$(CH_2)_{12}CH_3$, $(CH_2)_{15}CH_3$, 2×$(CH_2)_3CH_2NH_2$, $(CH_2)_3CH_2NHCO$), 2.93–2.98 (m, 4H; 2×CH_2NH_2), 3.08–3.56 (m, 9H; COC*H*(hexadecyl)CO, 4×CH_2NHCO), 3.87–3.99 (m, 2H; 2×C*H*NH_2CH_2), 4.22–4.28 ppm (m, 1H; COC*H*(NHCO)CH_2); ^{13}C NMR (125 MHz, $CDCl_3$/CD_3OD, 27°C): δ = 13.1, 20.9, 21.1, 22.0, 22.3, 25.9, 26.0, 26.3, 26.4, 26.76, 26.83, 27.7, 27.8, 28.7, 29.0, 29.9, 30.2, 30.9, 31.3, 38.0, 38.3, 38.4, 38.5, 38.9, 39.0, 52.4, 52.5, 52.8, 53.1, 53.4, 168.1, 168.5, 168.7, 170.3, 170.6, 171.0, 172.1, 172.2 ppm, MS: *m*/*z*: 950.7 $[M+H]^+$, 972.8 $[M+Na]^+$, 984.7 $[M+Cl]^-$, 948.7

$[M-H]^-$; HRMS calcd for $C_{53}H_{108}N_9O_5$ $[M+H]^+$: 950.8468; found: 950.8470.

N-*(2-{*N-*[(2*S*)-2,6-Diamino-1-oxohexyl]amino}ethyl)*-N′-*[6-(*N-*{(2*S*)-2,6-diamino-1-oxohexyl}amino-1-[*N-*(9*Z*)-octadec-9-enylamino]-1-oxohexan-(2*S*)-2-yl]-2-tetradecylpropandiamide (**lipid 3c**)*, $C_{55}H_{109}N_9O_5$: Yield: 82%; $R_f=0.24$ ($CHCl_3$/MeOH/NH_3, 50:50:10, v/v/v); ^{1}H NMR (500 MHz, $CDCl_3$, 27 °C): $\delta=0.88$ (t, ^3J(H,H) = 6.9 Hz, 6H; 2×CH_3), 1.24–1.88 (m, 68H; $NHCH_2(CH_2)_6CH_2CH{=}CHCH_2(CH_2)_6CH_3$, $(CH_2)_{13}CH_3$, 2×$(CH_2)_3CH_2NH_2$, $(CH_2)_3CH_2NHCO$), 1.96–2.03 (m, 4H; $CH_2CH{=}CHCH_2$), 2.70–2.74 (m, 4H; 2×CH_2NH_2), 3.01–3.06 (m, 1H; COC*H*(tetradecyl)CO), 3.17–3.46 (m, 10H; 4×CH_2NHCO, 2×$CHNH_2CH_2$]), 4.26–4.30 (m, 1H; COC*H*(NHCO)CH_2), 5.32–5.38 (m, 4H; C*H*=C*H*), 6.58–6.63/7.41–7.48/7.61–7.63/7.71–7.73 (4×m, 4H; 4×N*H*CO), 7.32 ppm (d, ^3J(H,H) = 7.8 Hz, 1H; COCH(N*H*CO)CH_2); ^{13}C NMR (125 MHz, $CDCl_3$/CD_3OD, 27 °C): $\delta=13.5$, 22.13, 22.17, 22.23, 22.52, 22.57, 26.56, 26.58, 26.8, 27.06, 27.08, 28.2, 28.3, 28.89, 28.93, 29.05, 29.08, 29.1, 29.24, 29.27, 29.33, 29.36, 29.68, 29.75, 30.11, 30.18, 30.3, 30.7, 31.2, 31.48, 31.50, 32.16, 34.18, 34.22, 38.2, 38.3, 38.4, 38.5, 38.7, 38.8, 39.18, 39.23, 40.0, 40.14, 40.17, 40.19, 53.1, 53.2, 54.3, 54.4, 129.3, 129.5, 170.65, 170.73, 170.9, 171.3, 171.9, 172.0, 175.59, 175.63, 175.9, 176.1 ppm; MS: *m/z*: 976.8 $[M+H]^+$, 489.0 $[M+2H]^{2+}$, 1010.7 $[M+Cl]^-$, 974.8 $[M-H]^-$; HRMS calcd for $C_{55}H_{110}N_9O_5$ $[M+H]^+$: 976.8624; found: 976.8628.

N-*[6-Amino-1-oxo-1-(*N-*tetradecylamino)hexan-(2*S*)-2-yl]*-N′-*{2-[*N,N-*bis(2-aminoethyl)amino]ethyl}-2-tetradecylpropandiamide (**lipid 4a**)*, $C_{43}H_{89}N_7O_3$: Yield: 97%; $R_f=0.09$ ($CHCl_3$/MeOH/NH_3, 65:35:5, v/v/v); ^{1}H NMR (500 MHz, $CDCl_3$, 27 °C): $\delta=0.89$ (t, ^3J(H,H) = 7.0 Hz, 6H; 2×CH_3), 1.24–1.92 (m, 56H; $NHCH_2(CH_2)_{12}CH_3$, $(CH_2)_{13}CH_3$, $(CH_2)_3CH_2NH_2$), 2.48–2.61 (m, 6H; $CH_2N(CH_2CH_2NH_2)_2$), 2.70 (dt, ^3J-(H,H) = 6.9, ^2J(H,H) = 14.0 Hz, 2H; $(CH_2)_3CH_2NH_2$), 2.75–2.79 (m, 4H; $CH_2N(CH_2CH_2NH_2)_2$), 3.03–3.41 (m, 5H; 2×CH_2NHCO, COC*H*(tetradecyl)CO), 4.31–4.41 (m, 1H; COC*H*(NHCO)CH_2), 6.69–6.71/7.38–7.42/8.18–8.20/8.32–8.33 ppm (4×m, 3H; 3×N*H*CO); ^{13}C NMR (125 MHz, $CDCl_3$/CD_3OD, 27 °C): $\delta=13.6$, 22.3, 22.4, 26.6, 27.13, 27.19, 28.92, 28.94, 28.98, 29.03, 29.05, 29.13, 29.15, 29.2, 29.3, 31.1, 31.3, 31.4, 31.6, 36.9, 38.3, 38.4, 39.18, 39.22, 40.5, 53.08, 53.12, 53.28, 55.34, 170.6, 170.8, 171.3, 171.7, 171.8 ppm; MS: *m/z*: 752.8 $[M+H]^+$, 377.1 $[M+2H]^{2+}$, 774.8 $[M+Na]^+$; HRMS calcd for $C_{43}H_{90}N_7O_3$ $[M+H]^+$: 752.7100; found: 752.7100.

N-*[6-Amino-1-oxo-1-(*N-*tetradecylamino)hexan-(2*S*)-2-yl]*-N′-*{2-[*N,N-*bis(2-aminoethyl)amino]ethyl}-2-hexadecylpropandiamide (**lipid 4b**)*, $C_{45}H_{93}N_7O_3$: Yield: 93%; $R_f=0.09$ ($CHCl_3$/MeOH/NH_3, 65:35:5, v/v/v); ^{1}H NMR (500 MHz, $CDCl_3$, 27 °C): $\delta=0.88$ (t, ^3J(H,H) = 7.0 Hz, 6H; 2×CH_3), 1.24–1.89 (m, 60H; $NHCH_2(CH_2)_{12}CH_3$, $(CH_2)_{15}CH_3$, $(CH_2)_3CH_2NH_2$), 2.53–2.60 (m, 6H; $CH_2N(CH_2CH_2NH_2)_2$), 2.67–2.77 (m, 6H; 3×CH_2NH_2), 3.07 (t, ^3J(H,H) = 7.6 Hz, 1H; COC*H*(hexadecyl)CO), 3.12–3.39 (m, 4H; 2×CH_2NHCO), 4.30–4.40 (m, 1H; COC*H*-(NHCO)CH_2), 6.69–6.71/7.36–7.38/8.29–8.30 ppm (3×m, 3H; 3×N*H*CO); ^{13}C NMR (125 MHz, $CDCl_3$/CD_3OD, 27 °C): $\delta=13.3$, 22.1, 22.39, 26.42, 26.96, 27.03, 28.76, 28.81, 29.0, 29.1, 29.2, 31.6, 31.3, 31.4, 31.5, 31.65, 31.69, 36.8, 36.9, 38.4, 38.99, 39.02, 40.5, 52.88, 52.92, 52.98, 55.8, 170.6, 170.8, 171.1, 171.59, 171.64 ppm; MS: *m/z*: 780.7 $[M+H]^+$, 391.1 $[M+2H]^{2+}$, 778.7 $[M-H]^-$; HRMS calcd for $C_{45}H_{94}N_7O_3$ $[M+H]^+$: 780.7413; found: 780.7413.

N-*{6-Amino-1-[*N-*(9*Z*)-octadec-9-enylamino]-1-oxohexan-(2*S*)-2-yl}*-N′-*{2-[*N,N-*bis(2-aminoethyl)amino]ethyl}-2-tetradecylpropandiamide (**lipid 4c**)*, $C_{47}H_{95}N_7O_3$: Yield: 81%; $R_f=0.30$ ($CHCl_3$/MeOH/NH_3, 65:35:5, v/v/v); ^{1}H NMR (500 MHz, $CDCl_3$, 27 °C): $\delta=0.75$ (t, ^3J(H,H) = 6.5 Hz, 6H; 2×CH_3), 1.11–1.69 (m, 56H; $NHCH_2(CH_2)_6CH_2CH{=}CHCH_2(CH_2)_6CH_3$, $(CH_2)_{13}CH_3$, $(CH_2)_3CH_2NH_2$), 1.83–1.88 (m, 4H; $CH_2CH{=}CHCH_2$), 2.32–2.45 (m, 6H; $CH_2N(CH_2CH_2NH_2)_2$), 2.52–2.56 (m, 6H; 3×CH_2NH_2), 2.90–3.31 (m, 5H; 2×CH_2NHCO, COC*H*(tetradecyl)CO), 4.26–4.31 (m, 1H; COC*H*(NHCO)CH_2), 5.20–5.24 (m, 2H; C*H*=C*H*), 7.15–7.86/8.02–8.10/8.14–8.24 ppm (3×m, 3H; 3×N*H*CO); ^{13}C NMR (125 MHz, $CDCl_3$/CD_3OD, 27 °C): $\delta=13.9$, 22.4, 22.67, 22.68, 26.71, 26.77, 26.9, 27.4, 27.5, 28.99, 29.05, 29.13, 29.21, 29.24, 29.36, 29.41, 29.45, 29.48, 31.59, 31.61, 31.68, 31.9, 32.16, 32.29, 36.7, 37.6, 39.2, 39.3, 39.38, 39.44, 41.45, 41.53, 52.8, 52.9, 53.0, 53.9, 54.2, 56.9, 57.1, 129.40, 129.61, 170.0, 170.4, 170.9, 171.0, 171.2, 171.4 ppm; MS: *m/z*: 807.4 $[M+H]^+$, 840.8 $[M+Cl]^-$, 804.9 $[M-H]^-$; HRMS calcd for $C_{47}H_{96}N_7O_3$ $[M+H]^+$: 806.7569; found: 806.7567.

Removal of the Boc protective group with hydrochloric acid (lipid 5a–c and lipid 6a–c):

Method a: The Boc-protected lipid (0.2 mmol) was suspended in acetic acid ethyl ester (15 mL). HCl (4 mL, 36%) was added stepwise within 2 h and the reaction mixture was stirred for 6 h. Then, the solvent was separated in vacuo. Ammonia (10 mL, 15%) was added carefully under stirring while cooling with an ice bath, and subsequently brine with K_2CO_3 (20%; 10 mL) was added to the suspension. The mixture was extracted three times with $CHCl_3$. The combined organic layers were washed with brine, dried over Na_2SO_4, filtered and the solvent was evaporated. The crude lipid was purified by column chromatography using silica gel 60 (2 g for 150 mg crude product) and $CHCl_3$/MeOH/NH_3 with the gradient technique.

Method b: The Boc-protected lipid (0.2 mmol) was suspended in acetic acid ethyl ester (15 mL). Over 2 h, HCl (4 mL, 36%) was added stepwise. The reaction mixture was stirred for 6 h, then the solvent was evaporated. The residue was dissolved in a mixture of $CHCl_3$ (4 mL) and methanol (1 mL), and DMAP (1.2 mmol, 146 mg) was added. This mixture was separated by column chromatography using silica gel 60 (2 g for 150 mg crude product) and $CHCl_3$/MeOH/NH_3 with the gradient technique to achieve the pure lipid as the free base.

N-*[6-Amino-1-oxo-1-(*N-*tetradecylamino)hexan-(2*S*)-2-yl]*-N′-*{2-[*N,N-*bis(2-{*N-*[(2*S*)-2,6-diamino-1-oxohexyl]amino}ethyl)amino]ethyl}-2-tetradecylpropandiamide (**lipid 5a**)*, $C_{55}H_{113}N_{11}O_5$: Yield: 69% (method a); $R_f=0.18$ ($CHCl_3$/MeOH/NH_3, 35:65:15, v/v/v); ^{1}H NMR (500 MHz, $CDCl_3$, 27 °C): $\delta=0.86$ (t, ^3J(H,H) = 6.7 Hz, 6H; 2×CH_3), 1.23–1.81 (m, 68H; $NHCH_2(CH_2)_{12}CH_3$, $(CH_2)_{13}CH_3$, 3×$(CH_2)_3CH_2NH_2$), 2.48–2.58 (m, 6H; $CH_2N(CH_2CH_2NH)_2$), 2.66–2.74 (m, 6H; 3×CH_2NH_2), 3.11–3.48 (m, 11H; 4×CH_2NHCO, COC*H*(tetradecyl)CO, 2×$CHNH_2CH_2$), 4.28–4.31 (m, 1H; COC*H*(NHCO)CH_2), 7.14–7.21/7.46–7.86 ppm (2×m, 5H; 5×N*H*CO); ^{13}C NMR (125 MHz, $CDCl_3$/CD_3OD, 27 °C): $\delta=13.2$, 22.06, 22.13, 22.3, 26.4, 26.94, 27.00, 28.76, 28.88, 28.92, 28.98, 29.1, 29.7, 30.1, 30.5, 30.6, 31.26, 31.34, 31.40, 34.2, 37.0, 37.1, 37.3, 39.0, 39.77, 39.83, 40.0, 52.8, 52.9, 53.3, 53.4, 53.5, 53.6, 54.1, 170.5, 170.7, 171.0, 171.6, 171.7, 172.1, 175.6, 175.7 ppm; MS: *m/z*: 1008.6 $[M+H]^+$, 1030.7 $[M+Na]^+$, 1042.6 $[M+Cl]^-$; HRMS calcd for $C_{55}H_{114}N_{11}O_5$ $[M+H]^+$: 1008.8999; found: 1008.9027.

N-*[6-Amino-1-oxo-1-(*N-*tetradecylamino)hexan-(2*S*)-2-yl]*-N′-*{2-[*N,N-*bis(2-{*N-*[(2*S*)-2,6-diamino-1-oxohexyl]amino}ethyl)amino]ethyl}-2-hexadecylpropandiamide (**lipid 5b**)*, $C_{57}H_{117}N_{11}O_5$: Yield: 58% (method a); $R_f=0.18$ ($CHCl_3$/MeOH/NH_3, 35:65:15, v/v/v); ^{1}H NMR (500 MHz, D_2O, 60 °C): $\delta=0.88$–0.89 (m, 6H; 2×CH_3]), 1.30–2.04 (m, 72H; $NHCH_2$-$(CH_2)_{12}CH_3$, $(CH_2)_{15}CH_3$, 3×$(CH_2)_3CH_2NH_2$), 2.91–3.01 (m, 6H; CH_2N-$(CH_2CH_2NH)_2$), 3.07–3.13 (m, 6H; 3×CH_2NH_2), 3.19–3.60 (m, 9H; 4×CH_2NHCO, COC*H*(hexadecyl)CO), 4.47 (t, ^3J(H,H) = 4.1 Hz, 2H; 2×$CHNH_2CH_2$), 4.35–4.40 ppm (m, 1H; COC*H*(NHCO)CH_2); ^{13}C NMR (125 MHz, D_2O, 60 °C): $\delta=14.0$, 21.9, 22.6, 22.7, 22.8, 26.7, 27.3, 27.5, 27.6, 29.5, 29.67, 29.76, 30.2, 30.89, 30.94, 31.15, 31.20, 31.8, 32.2, 36.8, 37.0, 37.2, 39.6, 39.8, 52.8, 53.0, 53.7, 54.0, 54.4, 170.40, 171.44, 171.6, 171.9, 172.5, 172.9, 173.2 ppm; MS: *m/z*: 1036.6 $[M+H]^+$, 1058.7 $[M+Na]^+$, 1070.6 $[M+Cl]^-$; HRMS calcd for $C_{57}H_{118}N_{11}O_5$ $[M+H]^+$: 1036.9312; found: 1036.9321.

N-*(6-Amino-1-{*N-*[(9*Z*)-octadec-9-enylamino]-1-oxohexan-(2*S*)-2-yl})*-N′-*{2-[*N,N-*bis(2-{*N-*[(2*S*)-2,6-diamino-1-oxohexyl]amino}ethyl)amino]ethyl}-2-tetradecylpropandiamide (**lipid 5c**)*, $C_{59}H_{119}N_{11}O_5$: Yield: 70% (method a); $R_f=0.19$ ($CHCl_3$/MeOH/NH_3, 35:65:15, v/v/v); ^{1}H NMR (500 MHz, $CDCl_3$, 27 °C): $\delta=0.88$ (t, ^3J(H,H) = 6.8 Hz, 6H; 2×CH_3), 1.25–1.88 (m, 68H; $NHCH_2(CH_2)_6CH_2CH{=}CHCH_2(CH_2)_6CH_3$, $(CH_2)_{13}CH_3$, 3×$(CH_2)_3CH_2NH_2$), 1.95–2.01 (m, 4H; $CH_2CH{=}CHCH_2$), 2.50–2.58 (m, 6H; $CH_2N(CH_2CH_2NH)_2$), 2.67–2.72 (m, 6H; 3CH_2NH_2), 3.12–3.36 (m, 11H; 4×CH_2NHCO, COC*H*(tetradecyl)CO, 2×$CHNH_2CH_2$), 4.28–4.32 (m, 1H; COC*H*(NHCO)CH_2]), 5.34–5.38 (m, 2H; C*H*=C*H*), 7.14–7.15/7.65–7.66/7.84–7.85 (3×m, 4H; 4×N*H*CO), 7.47–7.49 ppm (m, 1H; COCH(N*H*CO)CH_2); ^{13}C NMR (125 MHz, $CDCl_3$/CD_3OD, 27 °C): $\delta=13.8$, 22.38, 22.45, 22.51, 22.6, 26.8, 27.0, 27.32, 27.37, 28.6, 28.7, 29.0, 29.1, 29.25, 29.32, 29.5, 31.2, 31.3, 31.4, 31.7, 31.8,

32.4, 34.4, 34.7, 37.2, 37.3, 37.4, 37.5, 37.6, 39.3, 39.5, 40.4, 40.5, 40.6, 40.7, 53.1, 53.7, 53.8, 54.0, 54.2, 54.4, 54.5, 129.5, 129.8,, 170.6, 170.8, 171.0, 171.3, 171.7, 171.75, 175.71, 175.79, 175.9, 176.0 ppm; MS: *m/z*: 1062.7 $[M+H]^+$, 531.9 $[M+2H]^{2+}$, 1096.7 $[M+Cl]^-$; HRMS calcd for $C_{59}H_{120}N_{11}O_5$ $[M+H]^+$: 1062.9468; found: 1062.9473.

N-*{2-{*N,N-*Bis(2-{*N-*[(*2S*)-2,6-diamino-1-oxohexyl]amino}ethyl)amino}ethyl}*-N′-*(6-{*N-*[(*2S*)-2,6-diamino-1-oxohexyl]amino}-1-oxo-1-(*N*-tetradecylamino)hexan-(*2S*)-2-yl)-2-tetradecylpropandiamide (**lipid 6a**),* $C_{61}H_{125}N_{13}O_6$: Yield: 27% (method a), 99% (method b); $R_f=0.14$ ($CHCl_3$/MeOH/NH_3, 35:65:15, v/v/v); ^{1}H NMR (500 MHz, D_2O, 60°C): $\delta=0.87$–0.89 (m, 6H; $2\times CH_3$), 1.30–1.91 (m, 74H; $NHCH_2(CH_2)_{12}CH_3$, $(CH_2)_{13}CH_3$, $3\times(CH_2)_3CH_2NH_2$, $(CH_2)_3CH_2NHCO$), 2.71–2.78 (m, 6H; $CH_2N(CH_2CH_2NH)_2$), 3.08 (t, ^3J(H,H) = 7.5 Hz, 6H; $3\times CH_2NH_2$), 3.17–3.42 (m, 14H; $5\times CH_2NHCO$, $3\times CHNH_2CH_2$, COC*H*(tetradecyl)CO), 4.04 (t, ^3J(H,H) = 6.5 Hz, 3H; $3\times CHNH_2CH_2$); 4.31–4.36 ppm (m, 1H; COC*H*(NHCO)CH_2); ^{13}C NMR (125 MHz, $CDCl_3$/CD_3OD, 27°C): $\delta=$ 13.2, 21.3, 21.6, 22.0, 22.3, 26.05, 26.14, 26.17, 26.4, 26.92, 26.99, 27.9, 28.7, 28.9, 29.1, 30.3, 30.4, 31.3, 31.7, 31.8, 32.0, 37.2, 37.3, 37.4, 38.3, 38.5, 39.0, 52.9, 53.0, 53.1, 53.6, 53.7, 170.5, 170.6, 170.7, 171.8, 171.9, 172.0, 176.4 ppm; MS: *m/z*: 1136.6 $[M+H]^+$, 1158.8 $[M+Na]^+$, 1170.5 $[M+Cl]^-$; HRMS calcd for $C_{61}H_{126}N_{13}O_6$ $[M+H]^+$: 1136.9949; found: 1136.9958.

N-*{2-{*N,N-*Bis(2-{*N-*[(*2S*)-2,6-amino-1-oxohexyl]amino}ethyl)amino}ethyl}*-N′-*(6-{*N-*[(*2S*)-2,6-diamino-1-oxohexyl]amino}-1-oxo-1-(*N*-tetradecylamino)hexan-(*2S*)-2-yl)-2-hexadecylpropandiamide (**lipid 6b**),* $C_{63}H_{129}N_{13}O_6$: Yield: 97% (method b); $R_f=0.10$ ($CHCl_3$/MeOH/NH_3, 35:65:15, v/v/v); ^{1}H NMR (500 MHz, D_2O, 60°C): $\delta=0.86$–0.88 (m, 6H; $2\times CH_3$), 1.31–1.94 (m, 78H; $NHCH_2(CH_2)_{12}CH_3$, $(CH_2)_{15}CH_3$, $3\times(CH_2)_3CH_2NH_2$, $(CH_2)_3CH_2NHCO$), 2.71–2.74 (m, 6H; $CH_2N(CH_2CH_2NH)_2$), 2.83–2.85 (m, 6H; $3\times CH_2NH_2$), 3.17–3.42 (m, 14H; $5\times CH_2NHCO$, $3\times CHNH_2CH_2$, COC*H*(hexadecyl)CO), 4.34–4.37 ppm (m, 1H; COC*H*(NHCO)CH_2); ^{13}C NMR (125 MHz, D_2O, 60°C): $\delta=$14.0, 14.1, 22.7, 22.8, 22.9, 23.3, 27.3, 27.4, 27.5, 27.7, 28.8, 29.7, 29.9, 30.0, 30.2, 30.3, 30.8, 31.5, 32.17, 32.23, 34.7, 37.5, 37.6, 37.8, 37.9, 39.4, 39.7, 40.36, 40.41, 53.4, 53.5, 54.4, 55.1, 171.2, 171.3, 171.4, 173.1, 177.5, 177.6 ppm, MS: *m/z*: 1165.0 $[M+H]^+$, 1187.8 $[M+Na]^+$, 1163.1 $[M-H]^-$, 1199.0 $[M+Cl]^-$; HRMS calcd for $C_{63}H_{130}N_{13}O_6$ $[M+H]^+$: 1165.0262, found: 1165.0272.

N-*{2-{*N,N-*Bis(2-{*N-*[(*2S*)-2,6-diamino-1-oxohexyl]amino}ethyl)amino}ethyl}*-N′-*(6-{*N-*[(*2S*)-2,6-diamino-1-oxohexyl]amino}-1-{*N-*[(*9Z*)-octadec-9-enylamino]-1-oxohexan-(*2S*)-2-yl)-2-tetradecylpropandiamide (**lipid 6c**),* $C_{65}H_{131}N_{13}O_6$: Yield: 21% (method a), 97% (method b); $R_f=0.14$ ($CHCl_3$/MeOH/NH_3, 35:65:15, v/v/v); ^{1}H NMR (500 MHz, $CDCl_3$, 27°C): $\delta=0.88$ (t, ^3J(H,H) = 6.6 Hz, 6H; $2\times CH_3$), 1.25–1.88 (m, 74H; $NHCH_2(CH_2)_6CH_2CH{=}CHCH_2(CH_2)_6CH_3$, $(CH_2)_{13}CH_3$, $3\times(CH_2)_3CH_2NH_2$, $(CH_2)_3CH_2NHCO$), 1.94–2.03 (m, 4H; $CH_2CH{=}CHCH_2$), 2.54–2.59 (m, 6H; $CH_2N(CH_2CH_2NH)_2$), 2.68 (t, ^3J(H,H) = 5.3 Hz, 6H; $3\times CH_2NH_2$), 3.12–3.36 (m, 14H; $5\times CH_2NHCO$, $3\times CHNH_2CH_2$, COC*H*(tetradecyl)-CO), 4.28–4.32 (m, 1H; COC*H*(NHCO)CH_2), 5.33–5.39 (m, 2H; $CH{=}CH$), 7.18–7.21/7.41–7.44/7.55–7.58/7.66–7.68/7.83–7.86 ppm ($5\times$m, 6H; $6\times$N*H*CO); ^{13}C NMR (125 MHz, $CDCl_3$/CD_3OD, 27°C): $\delta=$13.5, 22.2, 22.6, 22.7, 26.6, 26.8, 27.2, 28.5, 28.5, 28.89, 28.94, 29.04, 29.09, 29.14, 29.3, 31.2, 32.15, 32.24, 32.3, 34.59, 34.66, 37.1, 37.3, 38.4, 39.2, 40.9, 52.9, 53.0, 53.3, 53.5, 53.6, 54.5, 54.6, 129.2, 129.4, 170.59, 170.63, 171.3, 171.4, 175.5, 175.6, 175.7 ppm; MS: *m/z*: 1190.9 $[M+H]^+$, 596.2 $[M+2H]^{2+}$, 397.8 $[M+3H]^{3+}$, 1212.9 $[M+Na]^+$, 1224.9 $[M+Cl]^-$; HRMS calcd for $C_{65}H_{132}N_{13}O_6$ $[M+H]^+$: 1191.0418, found: 1191.0427.

Sample preparation: The pure lipid was suspended in 10 mM carbonate buffer (pH 10, Na_2CO_3/$NaHCO_3$) to a concentration of 1 mg mL^{-1}. The samples were heated twice to 80°C and thoroughly mixed using a vortex, followed by 20 min of sonication at 60°C. Finally, the samples were degassed for 15 min.

DSC: The DSC measurements were performed on a MicroCal VP-DSC apparatus (MicroCal Inc., Northampton, MA, USA). The heating rate was 60 or 20 K h^{-1}, each heating and cooling scan was repeated to confirm reproducibility, and the first scan was disregarded. The observed temperature range was from 2 to 95°C. The reference cell was filled with pure solvent (carbonate buffer, pH 10). The buffer–buffer baseline was subtracted from the thermograms of the samples, and the DSC scans were evaluated by using MicroCal Origin 8.0 software.

DLS: The particle size was measured in carbonate buffer of pH 10 by photon correlation spectroscopy on a Zetasizer Nano-ZS ZEN3600 (Malvern Instruments Ltd., Malvern, Worcestershire, UK) with a sample refractive index of 1.33 and a viscosity of 0.8872 MPa s at 25°C. Every sample was measured three times. Each run consisted of 15 consecutive scans with a duration of 20 s. Results shown are the average of these three values. The correlation data were evaluated with ALV-Correlation software version 3.0 using an exponential regularised fit (see Supporting Information). We used a regularised exponential fit for the analysis of the correlation functions obtained because the commonly used cumulants analysis is restricted to monodisperse systems with radii between 30 and 100 nm.[36]

TEM: The samples were suspended with 10 mM carbonate buffer (pH 10, Na_2CO_3/$NaHCO_3$) to a final concentration of 0.05 mg mL^{-1} and were sonicated at 60°C for 10 min. The negatively stained samples were prepared by spreading 5 μL of the dispersion onto a Cu grid coated with a formvar film. After 1 min, excess liquid was blotted off with filter paper and aqueous uranyl acetate (1%, 5 μL) was placed onto the grid and drained off after 1 min. The dried specimens were examined with a Zeiss EM900 transmission electron microscope.

Acknowledgements

We thank Dr. Christian Ihling and Prof. Dr. Andrea Sinz (Institute of Pharmacy, Martin-Luther-University, Halle (Saale), Germany) for the high-resolution mass spectrometry analyses. The support of Dr. Gerd Hause (Biocenter, Martin-Luther-University, Halle-Wittenberg) by providing access to the electron microscope facility is greatly appreciated. Furthermore, we thank Tino Heimburg (Institute of Pharmacy, Martin-Luther-University Halle-Wittenberg) for the calculation of the energy minimized lipid structures.

[1] a) M. A. Mintzer, E. E. Simanek, *Chem. Rev.* **2009**, *109*, 259–302; b) S. Bhattacharya, A. Bajaj, *Chem. Commun.* **2009**, 4632–4656.
[2] C. R. Dass, P. F. M. Choong, *Cancer Cell Int.* **2006**, *6*, 17.
[3] a) C. Lonez, M. Vandenbranden, J.-M. Ruysschaert, *Prog. Lipid Res.* **2008**, *47*, 340–347; b) A. Joseph, N. Itskovitz-Cooper, S. Samira, O. Flasterstein, H. Eliyahu, D. Simberg, I. Goldwaser, Y. Barenholz, E. Kedar, *Vaccine* **2006**, *24*, 3990–4006; c) C. Barnier Quer, A. Elsharkawy, S. Romeijn, A. Kros, W. Jiskoot, *Eur. J. Pharm. Biopharm.* **2012**, *81*, 294–302.
[4] A. Kanazawa, T. Ikeda, T. Endo, *Antimicrob. Agents Chemother.* **1994**, *38*, 945–952.
[5] a) A. El-Aneed, *J. Controlled Release* **2004**, *94*, 1–14; b) T. P. O'Connor, R. G. Crystal, *Nat. Rev. Genet.* **2006**, *7*, 261–276.
[6] a) J. Li, L. Huang, *Nanomedicine* **2010**, *5*, 1483–1486; b) A. A. Metwally, I. S. Blagbrough, *Pharmaceutics* **2011**, *3*, 406–424; c) J. Sparks, G. Slobodkin, M. Matar, R. Congo, D. Ulkoski, A. Rea-Ramsey, C. Pence, J. Rice, D. McClure, K. J. Polach, E. Brunhoeber, L. Wilkinson, K. Wallace, K. Anwer, J. G. Fewell, *J. Controlled Release* **2012**, *158*, 269–276.
[7] See, http://www.wiley.com//legacy/wileychi/genmed/clinical/, *Vol. 2012*, Wiley, **2012**, Charts & Tables, Vectors.
[8] a) M. A. Kay, J. C. Glorioso, L. Naldini, *Nat. Med.* **2001**, *7*, 33–40; b) Y. Seow, M. J. Wood, *Mol. Ther.* **2009**, *17*, 767–777.
[9] L. Xu, T. Anchordoquy, *J. Pharm. Sci.* **2011**, *100*, 38–52.
[10] a) M. Heinze, G. Brezesinski, B. Dobner, A. Langner, *Bioconjugate Chem.* **2010**, *21*, 696–708; b) C. Wölk, M. Heinze, P. Kreideweiß, M. Dittrich, G. Brezesinski, A. Langner, B. Dobner, *Int. J. Pharm.* **2011**, *409*, 46–56.
[11] a) M. Dittrich, M. Bottcher, J. S. L. Oliveira, B. Dobner, H. Moehwald, G. Brezesinski, *Soft Matter* **2011**, *7*, 10162–10173; b) M. Dittrich, M. Heinze, C. Wölk, S. S. Funari, B. Dobner, H. Möhwald, G.

Brezesinski, *ChemPhysChem* **2011**, *12*, 2328–2337; c) M. N. Antipina, B. Dobner, O. V. Konovalov, V. L. Shapovalov, G. Brezesinski, *J. Phys. Chem. B* **2007**, *111*, 13845–13850.
[12] H. Lv, S. Zhang, B. Wang, S. Cui, J. Yan, *J. Controlled Release* **2006**, *114*, 100–109.
[13] a) T. G. Park, J. H. Jeong, S. W. Kim, *Adv. Drug Delivery Rev.* **2006**, *58*, 467–486; b) K. Luger, A. W. Mader, R. K. Richmond, D. F. Sargent, T. J. Richmond, *Nature* **1997**, *389*, 251–260.
[14] T. W. Green, P. G. M. Wuts in *Protecive Groups in Organic Synthesis*, 2nd ed., Wiley, **1991**, p. 318.
[15] T. H φeg-Jensen, M. H. Jakobsen, A. Holm, *Tetrahedron Lett.* **1991**, 32, 6387–6390.
[16] N. Zinieris, L. Leondiadis, N. Ferderigos, *J. Comb. Chem.* **2005**, *7*, 4–6.
[17] a) B. Dobner, P. Nuhn, A. Büge, *Z. Chem.* **1988**, *28*, 299–300; b) D. E. Floyd, S. E. Miller, *J. Am. Chem. Soc.* **1947**, *69*, 2354–2355; c) J. Haldar, P. Kondaiah, S. Bhattacharya, *J. Med. Chem.* **2005**, *48*, 3823–3831; d) C. Milite, S. Castellano, R. Benedetti, A. Tosco, C. Ciliberti, C. Vicidomini, L. Boully, G. Franci, L. Altucci, A. Mai, G. Sbardella, *Bioorg. Med. Chem.* **2011**, *19*, 3690–3701; e) P. L. Anelli, F. Montanari, S. Quici, G. Ciani, A. Sironi, *J. Org. Chem.* **1988**, *53*, 5292–5298; f) K. Prasad, H. Estermann, C.-P. Chen, O. Repic, G. E. Hardtmann, *Tetrahedron: Asymmetry* **1990**, *1*, 421–424.
[18] D. S. Breslow, E. Baumgarten, C. R. Hauser, *J. Am. Chem. Soc.* **1944**, *66*, 1286–1288.
[19] a) L. Fauconnot, F. Robert, R. Villard, F. Dionisi, *Chem. Phys. Lipids* **2006**, *139*, 125–136; b) E. Frérot, J. Coste, A. Pantaloni, M.-N. Dufour, P. Jouin, *Tetrahedron* **1991**, *47*, 259–270.
[20] G. W. Anderson, J. E. Zimmerman, F. M. Callahan, *J. Am. Chem. Soc.* **1964**, *86*, 1839–1842.
[21] G. L. Stahl, R. Walter, C. W. Smith, *J. Org. Chem.* **1978**, *43*, 2285–2286.
[22] F. Cavelier, C. Enjalbal, *Tetrahedron Lett.* **1996**, *37*, 5131–5134.
[23] M. Prashad, D. Har, B. Hu, H.-Y. Kim, M. J. Girgis, A. Chaudhary, O. Repič, T. J. Blacklock, W. Marterer, *Org. Process Res. Dev.* **2004**, *8*, 330–340.
[24] J. R. McDermott, N. L. Benoiton, *Can. J. Chem.* **1973**, *51*, 2562–2570.
[25] a) J. Coste, D. Le-Nguyen, B. Castro, *Tetrahedron Lett.* **1990**, *31*, 205–208; b) K. Prasad, K. Bharathi, B. B. Haseena, *Int. J. Pharm. Sci. Rev. Res.* **2011**, *8*, 108–119.
[26] W. E. Stewart, T. H. Siddall, *Chem. Rev.* **1970**, *70*, 517–551.
[27] a) M. Llinas, D. M. Wilson, M. P. Klein, *J. Am. Chem. Soc.* **1977**, *99*, 6846–6850; b) A. Blume, W. Huebner, G. Messner, *Biochemistry* **1988**, *27*, 8239–8249.
[28] D. Pawlowska, S. Tassler, G. Brezesinski, unpublished results.
[29] G. Cevc, *Biochemistry* **1991**, *30*, 7186–7193.
[30] G. Cevc, *Biochemistry* **1987**, *26*, 6305–6310.
[31] a) P. Garidel, C. Johann, A. Blume, *Biophys. J.* **1997**, *72*, 2196–2210; b) P. Garidel, C. Johann, A. Blume, *Eur. Biophys. J. Biophys.* **2011**, *40*, 891–905; c) R. N. A. H. Lewis, S. Tristram-Nagle, J. F. Nagle, R. N. McElhaney, *Biochim. Biophys. Acta Biomembr.* **2001**, *1510*, 70–82; d) K. Tada, K. Saito, M. Goto, N. Tamai, H. Matsuki, S. Kaneshina, *Biophys. Chem.* **2008**, *138*, 36–41; e) E. N. Serrallach, G. H. De Haas, G. G. Shipley, *Biochemistry* **1984**, *23*, 713–720.
[32] S. R. Sarker, S. Arai, M. Murate, H. Takahashi, M. Takata, T. Kobayashi, S. Takeoka, *Int. J. Pharm.* **2012**, *422*, 364–373.
[33] a) V. Gopal, J. Xavier, M. Z. Kamal, S. Govindarajan, M. Takafuji, S. Soga, T. Ueno, H. Ihara, N. M. Rao, *Bioconjugate Chem.* **2011**, *22*, 2244–2254; b) M. J. Blandamer, B. Briggs, P. M. Cullis, J. B. F. N. Engberts, R. I. Norman, *J. Chem. Soc. Faraday Trans.* **1996**, *92*, 3163–3164; c) A. Blume, *Biochim. Biophys. Acta Biomembr.* **1979**, *557*, 32–44; d) J. M. Boggs, *Biochem. Cell Biol.* **1986**, *64*, 50–57; e) J. M. Boggs, *Biochim. Biophys. Acta Rev. Biomembr.* **1987**, *906*, 353–404.
[34] P. R. Majhi, A. Blume, *J. Phys. Chem. B* **2002**, *106*, 10753–10763.
[35] J. Israelachvili, *Intermolecular and Surface Forces*, 2nd ed., Academic Press, San Diego, **1991**, p. 535–561.
[36] J. Pencer, F. R. Hallett, *Langmuir* **2003**, *19*, 7488–7497.

Received: December 20, 2012
Revised: June 25, 2012
Published online: August 9, 2013

